SYNTHESIS, STRUCTURAL AND PHOTOPHYSICAL PROPERTIES OF PHOSPHORESCENT OLIGONUCLEAR COMPLEXES OF MONOVALENT COINAGE METALS WITH NOVEL COMPOSITIONS

A THESIS

SUBMITTED IN PARTIAL FULFILLMENT OF THE REQUIREMENTS

FOR THE DEGREE OF MASTER OF SCIENCE

IN THE GRADUATE SCHOOL OF THE

TEXAS WOMAN'S UNIVERSITY

DEPARTMENT OF CHEMISTRY AND BIOCHEMISTRY

COLLEGE OF ARTS AND SCIENCES

BY

DANIEL KORIR B.ED.SC.

DENTON, TEXAS

DECEMBER 2013

TEXAS WOMAN'S UNIVERSITY

DENTON, TEXAS

08/15/2013

To the Dean of Graduate School:

I am submitting herewith a thesis written by Daniel Korir entitled "Synthesis, Structural and photophysical properties of phosphorescent Oligonuclear complexes of monovalent coinage metals with novel compositions." I have examined this thesis for form and content and recommend that it be accepted in partial fulfillment of the requirements for the degree of Master of Science with a major in Chemistry.

Manal Rawashdeh-Omary

Dr. Manal Rawashdeh-Omary, Major Professor

We have read this thesis and recommend its acceptance

Mark Ball

Manal Rawashdeh-Omary

Department Chair

Accepted:

Intern-Dean of the Graduate School

ACKNOWLEDGEMENTS

I must start by thanking the Lord God Almighty for the grace that was sufficient to see me through this long journey. My deep gratitude goes to Dr. Manal Rawashdeh-Omary, my advisor whose help, guidance, insight, patience, encouragement, mentorship and wisdom enriched my scientific experience immensely. My special thanks go to my advisory committee members; Dr. Richard Sheardy (Chair) and Dr. Mark Britt for their constant support during this long journey. I would like to thank the Omary group members; Ruaa Almotawa and Waheda Hassen for the help and support. I am greatly indebted to Dr. Mohammed Omary from UNT for allowing me to use his lab. Special thanks go to Omary group members at UNT specifically Dr. Ravi Arvapally and Gustavo Salazar. My sincere gratitude goes to the crystallographer at UNT Dr. Vladimir Nesterov for the help and support.

I must not forget to thank my family who put so much trust in me and constantly encouraged me particularly my mom, Rael Bet, paternal uncles Julius Bett and Jeremiah Bett. My brother Justus and sisters Luiza, Lily and Phyllis have been a great encouragement. Last but by no means the least my fiancé and wife to be; Susan Chesire for being so pivotal in encouraging, loving and motivating me throughout this noble endeavor.

ABSTRACT

DANIEL KORIR B.ED.SC.

SYNTHESIS, STRUCTURAL AND PHOTOPHYSICAL PROPERTIES OF PHOSPHORESCENT OLIGONUCLEAR COMPLEXES OF MONOVALENT COINAGE METALS WITH NOVEL COMPOSITIONS

DECEMBER 2013

This thesis is a study of monovalent coinage metal complexes made of small molecules and metallopolymers. It has 54pp, 1 table, 38 figures and the references for organometallic and metallopolymers of group 11 elements. It discusses four main chapters describing the synthesis; structure and photophysical studies of luminescent small molecules and metallopolymers of gold (I), Silver (I) and copper (I). Chapter one discusses the introduction to photophysics, coordination and spectroscopy of luminescent novel gold (I) silver (I) and copper (I) complexes. The second chapter involves synthesis, structural and photophysical studies of highly phosphorescent Au (I) small molecules and metallopolymers. Chapter three involves synthesis, structure and photophysical studies of Au (I) and Ag (I) mixed metal pyrazolate complexes. The fourth chapter discusses the study of the photophysical properties of new hydrogenless copper (I) and silver (I) pyrazolate complexes toward potential use as luminescent sensors for Volatile Organic Compounds (VOC) and other environmental pollutants.

TABLE OF CONTENTS

LIST OF TABLES

LIST OF FIGURES

CHAPTER I

CHEMISTRY OF COINAGE METAL COMPLEXES

This thesis covers a study of synthesis, spectroscopy and photophysics of d^{10} coinage metal complexes and polymers. Section 1.1 describes the introduction to coordination chemistry and spectroscopy of coinage metal complexes. Section 1.2 discusses the photophysics of complexes of d^{10} elements. In section 1.3, we discuss the spectroscopic advantages of luminescent metal complexes and metallopolymers.

1.1 Photophysics of Complexes of d^{10} Elements

The history of luminescence dates back to late 1880s when a German physicist Weidemann used it to refer to the kind of light not associated with rise in temperature[1]. He was able to identify different types of luminescence including photoluminescence. Photoluminescence occurs when an electron in the low energy ground state absorbs a discrete quantity of light at a given wavelength causing it to rise to a higher electronic state, called the excited state. If this electron falls back to the ground state, it undergoes a series of transitions both radiative and non-radiative. The radiative transition is referred to as photoluminescence.

After the first report on luminescent gold (I) complexes was made in 1970 by Dori, et al, extensive studies and use of luminescent gold (I) complexes and other d^{10} complexes has been growing very rapidly [2]. Complexes of group 11 elements have attracted significant interest in part because of their fascinating emissive properties[3] useful in fabrication of

optoelectronic devices[4] and partly because they can form discrete dinuclear, trinuclear, tetranuclear, polymeric units and clusters that have unique photonic applications[(5)]. Trinuclear gold (I) complexes for instance have attracted greater attention because they have great luminescence properties with long life times and tunable emissions through the visible region and because of their high potential for optoelectronic applications[6] such as Polymer light emitting diodes (PLEDs). The process of PLEDs development has evolved through the years with Rawashdeh-Omary and co-workers designing a phosphorescent Au-based Metallopolymer by directly coordinating a polymer such as poly-4vinylpyridine (PVP) to gold (I) precursors in an attempt to overcome the need for doping as was the case previously [7-8]. A high quality PLED will have such properties as strong luminescence with long lifetimes and high quantum yield, very soluble for easier film coating and lighting displays, stable under operating device conditions and low driving voltages.

The nature of emissive properties and electronic structure of gold (I) complexes makes some of them suitable for use in a myriad other applications. For instance, one of the treatments of Rheumatoid Arthritis is gold (I) complex[9], while others have industrial applications of interest to scientists as biosensors[10], photocatalysts [11] lasers and selective sensors for organic compounds such as Volatile organic Compounds[12].

Coordination of d^{10} elements such as Gold, silver and Copper with different ligands provide an avenue to understanding their chemistry including supramolecular structures, Metal-metal interaction, metallophilic bonding, metalloaromaticity and acid-base reactions[13]. It has been shown for example that the photophysical properties of gold are

attributed to the nature of the ligand, the supramolecular geometry of the ligands around the metal center and Metal-metal interractions[14]. Other factors that have a great influence on the photophysical properties are concentration, temperature, nature of the solvent used and the excitation wavelength[15 (a), b), (c)]. The nature of the luminescence of these complexes makes them excellent candidates for many types of applications as sensors for bioinorganic and organic compounds[16].

In order for a gold (I) complex to exhibit luminescence, there are key properties that the complex has to meet in order to show emission; including nature of the ligand, the geometry around the metal center and the M-M interactions[17-18].

Different tunable luminescence of the complexes of d^{10} elements have been achieved by changing the ligand (or substituent groups), metal center, solvent or the temperature[19]. Other reports on heterometallic centers with interesting emissive properties have also been the center of focus in the recent past, largely because it sheds light on the heterometallic attractions[20] of the coinage metal centers.

Rawashdeh-Omary and coworkers have demonstrated the rich spectroscopic and photophysical properties done by varying the metal center in trinuclear monovalent coinage metal complexes in an effort to obtain tunable photoluminescence in steady state and upon exposure to a Volatile Organic Compounds (VOCs) [21-22].

1.2 Coordination Chemistry and Spectroscopy of Group 11 Complexes

Different studies show that closed d^{10} systems such as silver (I) and gold (I) easily form oligomeric structures[23-25]. The overall heavy metal interaction, as is the case in d^8 or d^{10} coinage systems is either due to metallophilic interactions also referred to as M-M

interactions or the van der Waals attraction[26-27]. The metallophilic interactions may be intermolecular or intramolecular. Experimental data obtained from crystallographic measurements may be used to explain the strength of this attraction[28-29]. Au-Au interactions for instance have bonding comparable to hydrogen bonds which are relatively stronger than van der Waals bonds, but weaker than ionic or covalent bonds[30-31]. To determine whether M-M interactions exist in coordination of group 11 compounds, van der Waals values are used. The sum of the atomic radii of the coinage metal cations involved has to be less than the sum of the van der Waals radii of two metal cations usually less than 3.6Å for aurophilic attractions.

Pyykko hypothetically attributed these attractive forces to relativistic effects and dispersive interactions providing extra strength to the complex[32]. Attraction between the Au (I) ion and the d^{10} shell has been known to greatly contribute to the highly luminescent properties of gold moieties[33].

1.3 Luminescent Materials and their Spectroscopic Advantages

After Rawashdeh-Omary and co-workers made soluble oligomers with remarkable tunable luminescence across the UV-Visible region through systematic variation in temperature, concentration, and solvent and excitation wavelength[34-35], research has been focused on synthesis of coinage metal based polymers with better stability, solubility and tunable photophysical properties[36]. Solubility of new materials for instance has to combine superior quality of the polymer and the functionality provided by the presence of coinage metal centers.

Therefore, the understanding of this type of chemistry could allow the synthesis of complexes with appropriate metals and ligands tailored for individual applications such as superconductors, luminescent materials, biological catalysis and electrochromic materials that make metallopolymers better than their organic counterparts due to their two or three dimensional structures[37-38]. On the other hand, metallopolymers are preferred to small molecules in large scale device fabrication of luminescent materials because they can be easily processed over a large surface area using such methods as ink-jet printing and spin-coating. The presence of the heavy metal center as the polymer back-bone provides better structural stability and efficient phosphorescence through the intersystem crossing[39-40].

CHAPTER II

THE SYNTHESIS AND CHARACTERIZATION OF VARIOUS MONOVALENT GOLD (I) SMALL MOLECULES AND METALLOPOLYMERS

This chapter entails the synthesis, characterization and spectroscopic measurements of various small molecules and metallopolymers of monovalent gold (I). The synthesis involves direct coordination of labile gold (I) moieties with different σ-donors forming small molecules and metallopolymers with fascinating tunable phosphorescence. Section 2.1 covers a description of different instruments used for the characterization. In this section, we also present a description of chemicals and materials used to synthesize different gold (I) complexes. In section 2.2, a detailed synthetic method for gold (I) complexes is discussed while in section 2.3; the synthesis of gold (I) metallopolymers is covered. Section 2.4 discusses the spectroscopic measurements of gold (I) complexes. Lastly, section 2.5 is a summary of key findings and future prospects of the project.

2.1. Instruments, Chemicals and Materials

All the reactions were carried out using standard schlenk techniques under inert atmosphere using purified nitrogen. 1,2-bis(4-pyridyl)ethane (**bpa**) (I), 1,3-bis(4-pyridyl) propane (**bpp**) (II), trans-1,2-bis(4-pyridyl)ethylene (**bpe**) (III), 4,4-dipyridyl(**dipy**)(IV), piperazine(**ppz**) (V) and poly-4-vinylpyridine (**PVP**) (AMW=60,000) were purchased from sigma Aldrich and were used as received. Dichloromethane (DCM) was purchased

from Fisher scientific and was used after drying using molecular sieves. The following is a list of the ligands used as starting materials:

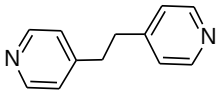

1,2-bis(4-pyridyl)ethane (**bpa**)

(I)

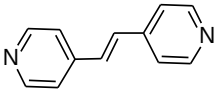

trans-1,2-bis(4-pyridyl)ethylene (**bpe**)

(II)

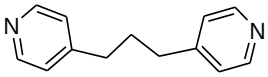

1,3-bis(4-pyridyl)propane (**bpp**)

(III)

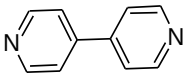

4,4-dipyridyl (**dipy**)

(IV)

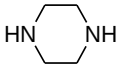

piperazine (**ppz**)

(V)

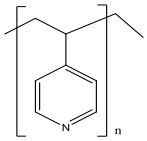

Poly-4-vinylpyridine (**PVP**)

Steady state photoluminescence was done using PTI (Photon Technology International) QuantaMaster Model QM-3/2006SE Scanning Spectrofluorometer equipped with a 75W xenon lamp, excitation and emission monochromators, excitation correction unit and PMT (Photomultiplier Tube) detector. The excitation spectra were corrected for wavelength-dependent lamp intensity while the emission spectra were also corrected for detector wavelength response. Temperature-dependent emission at 77K was done using liquid nitrogen as a coolant. Lifetime measurements were acquired using a high speed pulsed xenon lamp source interfaced to the PTI instrument along with an autocalibrated "Quadrascopic" monochromators for excitation wavelength selection. The ^{1}HNMR spectra were obtained using Varian Mercury 500Mhz NMR spectrometer. The chemical shifts given as ξ values in parts per million (ppm) from tetramethylsilane (TMS) as internal standard. Infrared (IR) spectra were obtained using Nicolet 6700 Fourier Transform- Infrared (FT-IR) spectrometer. Thermogravimetric Analyzer (TGA) was determined using TA Q500 TGA, equipped with high sensitivity auto sampler and dual

digital mass flow metering controllers. TGA was done in an inert environment using nitrogen and a heating rate of 25°C/minute. All compounds were heated from 30°C to 700°C. Melting points were obtained using Mel-tem capillary melting point apparatus. Elemental analysis was done by Intertek using Inductively Coupled Plasma Optical Emission Spectrometry (ICP-OES) methodology.

2.2 Synthesis of Gold (I) Complexes

*2.2.1 Synthesis of ClAubpa **(I)***

ClAuTHT + bpa $\longrightarrow$ ClAubpa

The main precursor, gold (I) tetrahydrothiophene chloride (ClAuTHT*)* was synthesized according to a literature procedure[41-43]. In all the reactions, standard schlenk technique is applied unless otherwise stated. 10 ml of DCM in a schlenk tube is degassed by passing a stream of purified nitrogen for 20 minutes under ice bathe. ClAuTHT (*0.034g, 0.106mmol*) is added and stirred for another 10 minutes or till it completely dissolves followed by bpa (0.02g, 0.108mmol). The reaction is stirred for 30 minutes under ice bathe followed by another 30 minutes at ambient temperatures. Black/Purple impurities are removed by vacuum filtration over a bed of cellite and washed with DCM. The solvent is then removed by vacuum to obtain a white solid, Melting point (M.P.) 126^{0}C (yields of 91 %.) Elemental analysis done showed C= 32.31%, N= 5.28%, H= 2.75%, Cl= 8.92%, Au= 45.87% with a marginal experimental error of 4.87%. This corresponds with the empirical formula $C_{12}H_{12}N_2AuCl$ (ClAubpa). The IH NMR (500Mz in CD_2Cl_2) δ 8.5, 7.1 (-CH in Pyridine ring), 2.9(-CH_2) The FTIR ν = 2210cm^{-1} (C=N), ν = 3040cm^{-1} (C-H aromatic), ν = 2900cm^{-1} (C-H aliphatic)

2.2.2 Synthesis of ClAubpe ***(II)***

ClAuTHT +bpe $\longrightarrow$ ClAubpe

The synthesis of (II) was done following procedure in (I) above by reacting 0.019g (0.104mmol) of bpe and stoichiometric quantity of ClAuTHT. The reaction immediately formed a light yellow precipitate. The product is obtained by vacuum filtration, washed with DCM and further dried by vacuuming for 2 hours. A light yellow solid is obtained with M.P. of 145^0C at a yield of 93%. The FT-IR ν = 2210cm^{-1}(C=N), ν = 3040cm^{-1} (C-H aromatic), ν = 2900cm^{-1} (C-H Aromatic)

2.2.3 Synthesis of ClAubpp ***(III)***

ClAuTHT +bpp $\longrightarrow$ ClAubpp

The procedure used in (I) above was followed using 0.05g (0.156mmol) of ClAuTHT and 0.031g (0.16mmol) of bpp. A cloudy white precipitate is formed immediately. The solvent is removed by filtration to obtain a white solid with M.P. 120^0C. The FT-IR ν = 1800cm^{-1}(C=N), ν = 3050cm^{-1} (C-H aromatic), ν = 2900cm^{-1} (C-H aliphatic), ν =2850CM^{-1} (C-H)

2.2.4 Synthesis of ClAudipy ***(IV)***

ClAuTHT +dipy $\longrightarrow$ ClAudipy

The procedure used for synthesis of (I) was followed. 0.05g (0.156mmol) of ClAuTHT is dissolved in DCM followed by 0.025g (0.156mmol) of dipy and stirred for 30 minutes. A cloudy white precipitate formed which was then removed by vacuum to obtain white

solid at 75% yield which decomposes at 95-100^{0}C.). ^{1}H NMR (500MHz. CD_2Cl_2) δ 7.5, 8.5 (C-H py)

2.2.5 Synthesis of ClAuppz ***(V)***

ClAuTHT +ppz ⟶ ClAuppz

This compound was synthesized using the procedure in (I). ClAuTHT (0.05g 0.156mmol) was dissolved in 10ml DCM followed by ppz (0.013g, 0.151mmol). The reaction was stirred for 30 minutes under ice bathe and another 1 hour at room temperature after which the solvent was removed by vacuum to obtain a white solid (Yield 71%). The FT-IR ν = 3220cm^{-1}(C-H stretch aromatic), ν = 2990cm^{-1} (C-H Stretch aliphatic), ν = 1490cm^{-1} (C-H Bend)

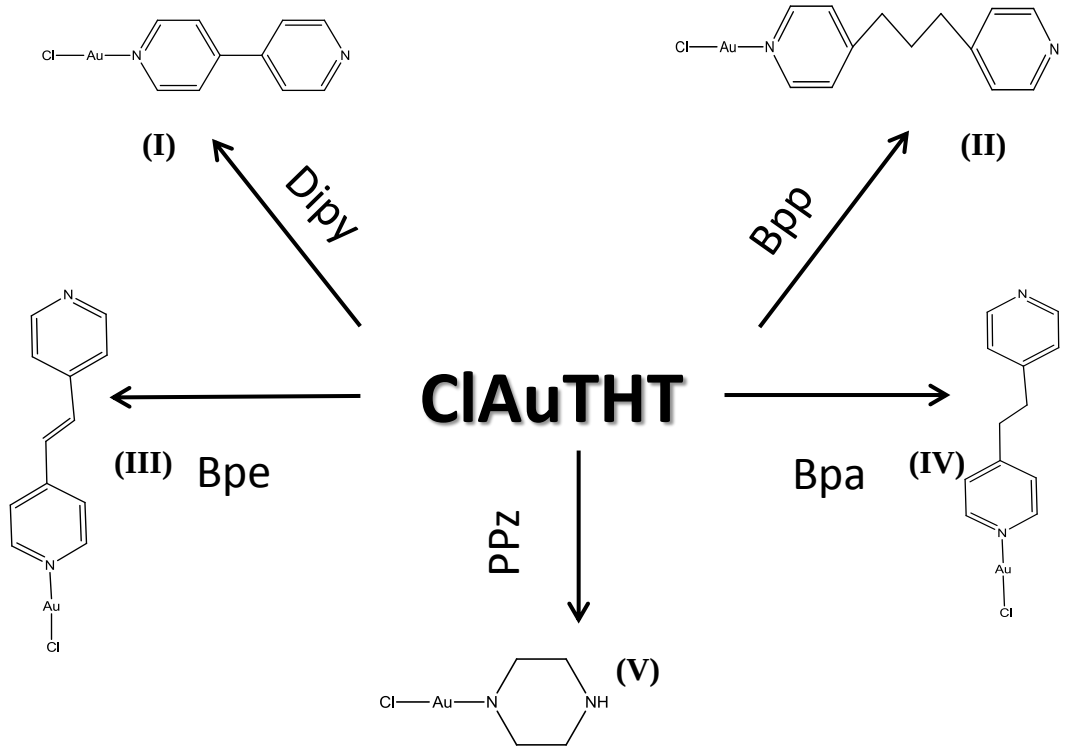

Figure1: Schematic representation and illustration of synthetic routes and coordination of gold (I) to different ligands.

2.3 Synthesis of Gold (I) Metallopolymers

2.3.1 Synthesis of bpaAu(PVP)$_n$ Cl

Metallopolymer bpaAu(PVP)$_n$Cl was prepared by dissolving stoichiometric amounts of ClAuTHT (0.05g, 0.156mmol), bpa (0.03g, 0.162mmol) and PVP(0.015g, 0.161mmol) (MW=60,0000) in 10 ml of DCM and stirring for 2 hrs following the procedure used in section 2.2.1. The solution turned white after about 10 minutes of stirring. The solvent was removed by vacuum to obtain a white solid with M.P. 208^{0}C.

2.3.2 Synthesis of bpeAu(PVP)$_n$Cl

Synthesis of bpeAu(PVP)$_n$Cl was done by degassing 10ml of DCM in a schlenk flask followed by equimolar amounts of the starting materials bpe (0.019g, 0.104mmol) and PVP (0.01g, 0.104mmol). Once complete dissolution occurred, ClAuTHT (0.034g, 0.104mmol) was added then stirred for 2 hours under ice bathe. It immediately formed light yellow precipitate which was removed by vacuum filtration, washed with DCM then dried to obtain a white solid (M.P =180^{0}C). The FT-IR ν = 1610cm^{-1}(C=N), ν = 2990cm^{-1} (C-H aromatic), ν =2850CM^{-1} (C-H Stretch aliphatic)

2.3.3 Synthesis of bppAu(PVP)$_n$Cl

The synthesis was done using the procedure in 2.3.2 using bpp (0.031g 0.156mmol) and PVP (0.015g 0.156mmol) in DCM. Upon complete dissolution, ClAuTHT (0.05, 0.156mmol) was added and stirred for 30 minutes under ice bathe. It turned cloudy white. The solvent was removed by vacuum to obtain a white solid (M.P 105^{0}C). The FT-IR ν = 1820cm^{-1}(C=N), ν = 2990cm^{-1} (C-H aromatic), ν = 2800cm^{-1} (C-H Aliphatic).

2.3.4 Synthesis of dipyAu(PVP)$_n$Cl

Synthesis was done following procedure in 2.3.2 using DCM as the solvent. 0.025g (0.16mmol) of dipy and PVP (0.015g, 0.16mmol) were added and stirred for 30 minutes under ice bathe. The reaction turned cloudy after 30 minutes. The reaction was allowed to proceed for another 30 minutes at room temperature, after which the solvent was removed by vacuum to obtain white solid. (M.P=145^{0}C)

2.3.5 Synthesis of ppzAu(PVP)$_n$Cl

The synthesis was done using the procedure in 2.3.2 using equimolar amounts of all the starting materials: ppz (0.013g, 0.151mmol), PVP (0.015g, 0.16mmol) and ClAuTHT (0.05, 0.156mmol). The reaction formed a cloudy precipitate after 10 minutes. The reaction progressed for another 30-45 minutes before the solvent was removed by vacuum and dried for 2 hours.

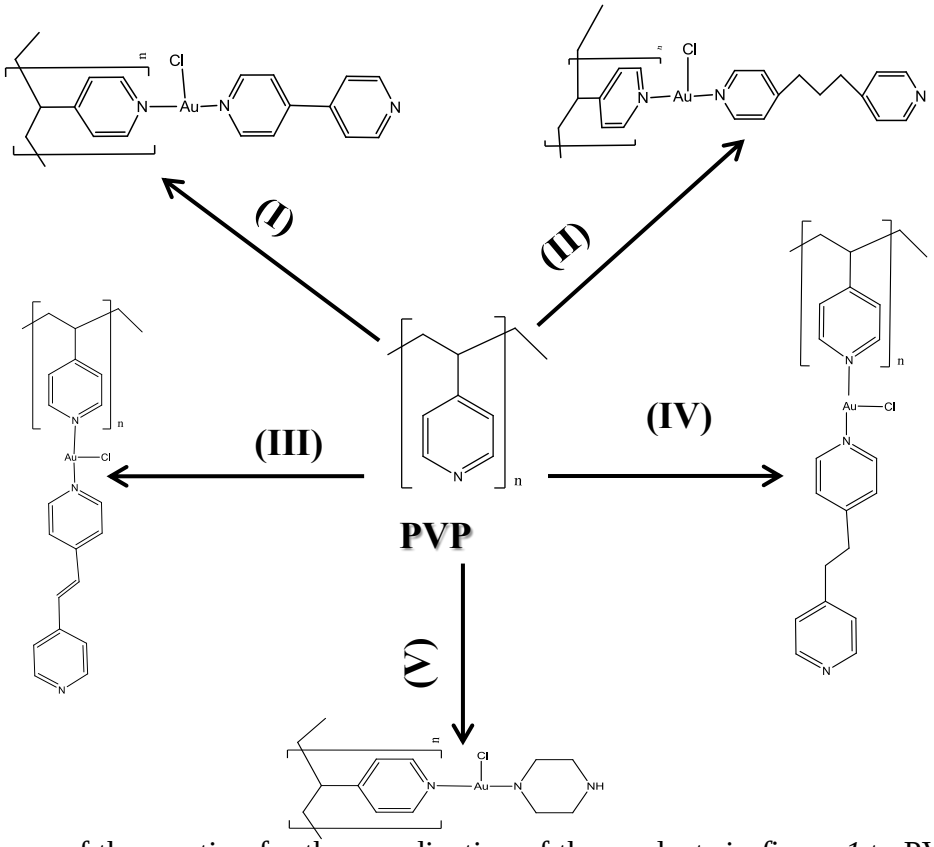

Figure 2*:* Scheme of the reaction for the coordination of the products in *figure 1* to PVP showing one of the possible products of the metallopolymer.

2.4 Results and Discussions

This study presents the findings on the structural motifs and photophysical properties of small molecules of gold (I) Compounds **I-V** (figure1) and their metallopolymers. Coordination easily occurs with each σ-donor used leading possibly to ligand to metal charge Transfer (LMCT) transition. The chloride on the other hand is considered both σ- and π-donor also forming LMCT transition. We used IR, TGA and elemental analysis values to predict the composition of the gold (I) complex. Figure 4 represents the TGA profile for ClAubpa (a), ClAuppz (b) and the metallopolymer bpeAu$(PVP)_n$Cl (c). Figure

4 (a) represents the weight loss for ClAubpa which shows a total ligand loss of 52.08%, and the gold residue at 47.92%. The elemental analysis on this sample showed that Au= 45.87%, C=32.31%, N=5.28%, H= 2.75%, Cl= 8.92% (error 4.87%). This data showed that the TGA and elemental analysis values are in agreement with the theoretical calculations (C=34.56%, Cl= 8.52%, N= 6.72%, H= 2.88%, Au= 47.27%) for the empirical formula $C_{12}H_{12}N_2AuCl$ (ClAubpa) within the experimental error of 5%. Figure 4(b) for ClAuppz showed total ligand and gold composition of 38.5% and 61.5% respectively verses the theoretical values of 39.2% and 61.8% respectively. In Figure 4(c), gold content constitutes 36.11% as compared to the theoretical value of 44.2% with about 8% experimental error. Based on these data sets, and molar ratio of the starting materials, we deduced the empirical formula to be ClAubpa (a), ClAuppz (b) and dipyAu$(PVP)_n$Cl (c) respectively. We used TGA only to predict the formula of the other complexes and metallopolymers since the theoretical TGA values are in agreement with those of ClAubpa. The residual material had golden yellow color which is consistent with the metallic element gold.

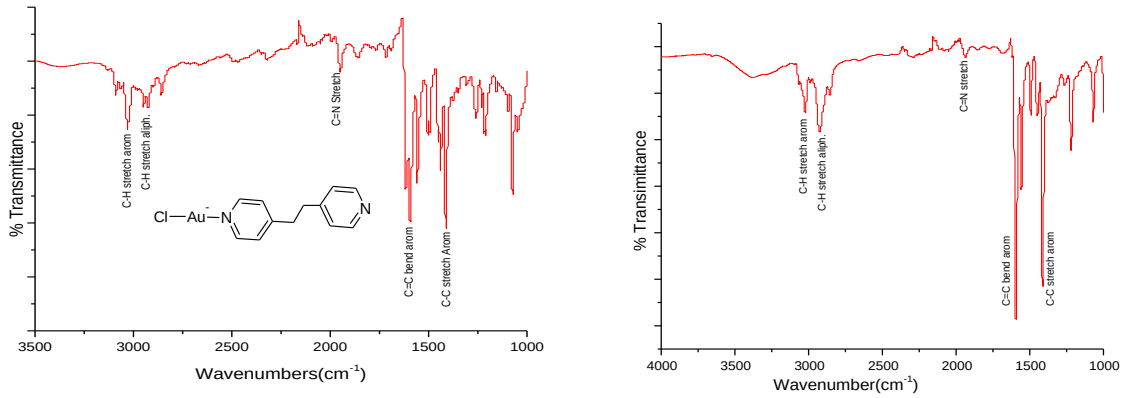

(a) *(b)*

Figure 3: The IR spectra for ClAubpa and bpaAu(PVP)$_n$Cl confirming the presence of the ligands in the product *for* (a) ClAubpa and (b) bpaAu(PVP)$_n$Cl

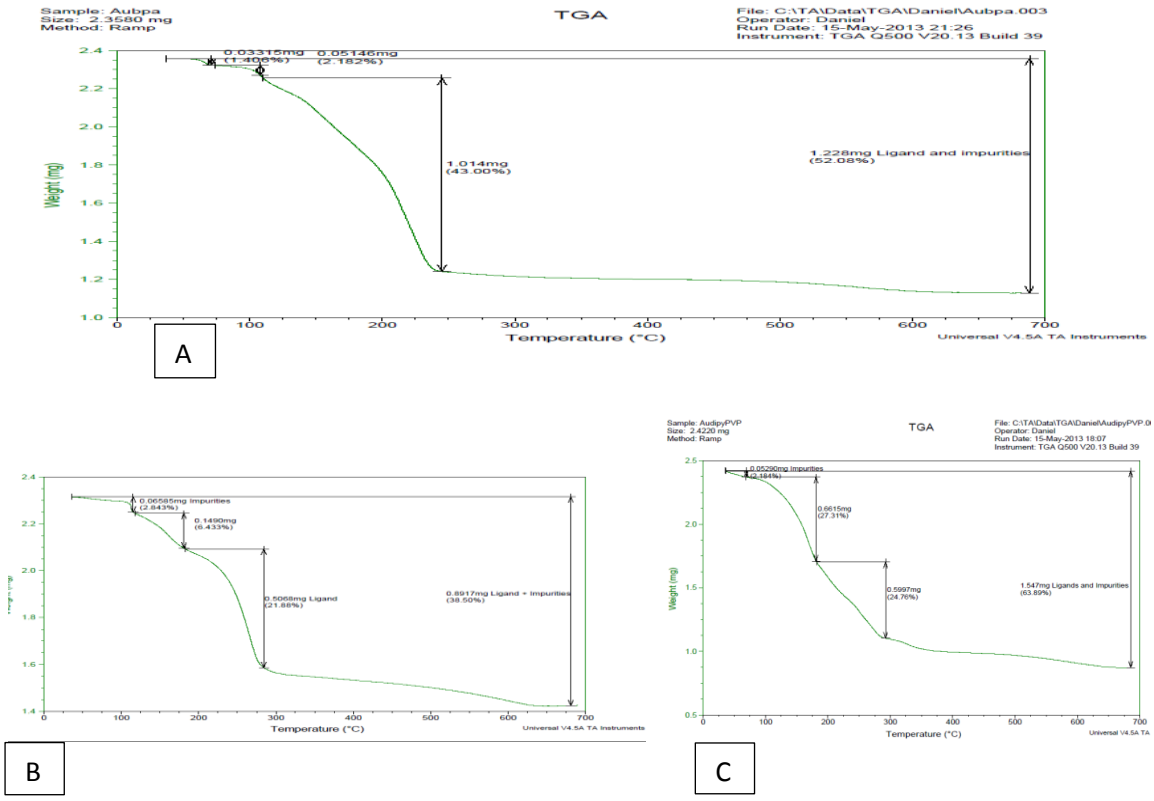

Figure 4: The TGA measurements of ClAubpa (a) ClAuppz (b) and the metallopolymer, dipyAu(PVP)$_n$Cl (c).

^{1}HNMR data for ClAubpa and ClAudipy using CD_2Cl_2 as reference are shown in figures 5 and 6 respectively. In figure 5, there are three distinct peaks at 8.5 ppm, 7.1ppm and 3.0ppm for ClAubpa. The peak downfield at 8.5ppm corresponds with the C-H (N-py) while the 7.1ppm peak represents C-H (C-py). The strong 3.0ppm peak matches the protons for the ethane bridge. In figure 6, there are two distinct peaks for the bipyridine protons at 8.5ppm representing the C-H (N-py), and 7.5ppm representing C-H (C-py). In both cases, the peaks suggest successful coordination of gold (I) to pyridine units. We were not able to obtain proton NMR data for the other samples due to very weak or no solubility of the products.

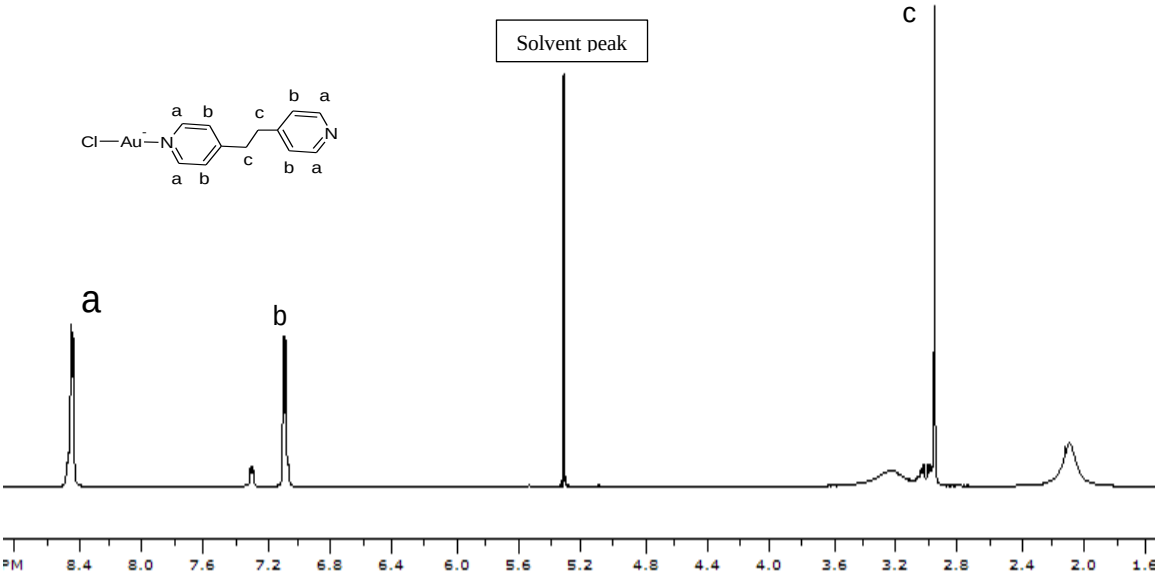

Figure 5: ^{1}HNMR for ClAubpa in CD_2Cl_2.

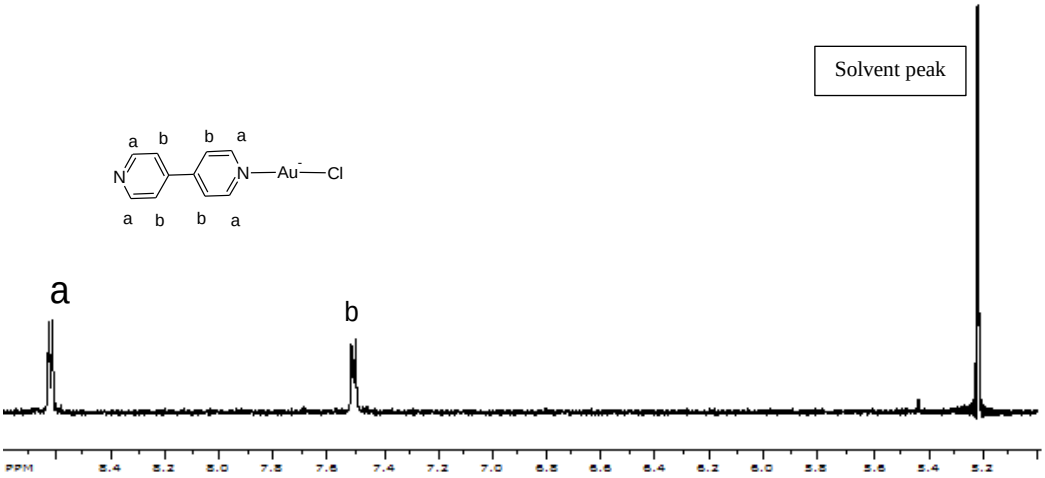

Figure 6*:* The data shows the ^{1}HNMR ClAudipy in CD_2Cl_2

Figure 7 shows the photoluminescence excitation and emission spectra for ClAubpa at room temperature (RT) with strong red emission (λ_{max}=692nm). Figure 8 represents the excitation and emission spectra for ClAubpa at 77K. The emission does not shift upon cooling to 77K but becomes more resolved with two peaks at 440nm and 991nm producing a white emission. No further tuning is seen upon changing the excitation wavelength. Figure 9 and 10 show the photoluminescence excitation and emission spectra for bpaAu$(PVP)_n$Cl at RT and 77K respectively. In figure 9 bpaAu$(PVP)_n$Cl exhibits blue emission at 430nm at RT. Upon cooling to 77K, the emission is red shifted to 471nm using 340nm excitation and is further red shifted to 496nm using 360nm excitation. Figures 11 and 12 represent the solid state photoluminescence excitation and emission spectra for ClAubpa at RT and 77K respectively. The ClAubpp exhibits intense emission at λ_{max}=791nm while upon cooling to 77K, slightly red shifted to 805nm producing bright white emission with better resolution producing two more lower energy emission bands

at 400nm and 560nm. ClAubpa and ClAubpp show a rather similar emission profile at 77K as shown in figures 7 and 11 respectively indicating high and low energy emission bands. ClAubpa (Figure 7) shows two separate emission bands: the low energy emission band at 440 nm and the high energy emission band at 691nm showing a bright white emission while ClAubpp has three emission bands at 400nm, 560nm and 805nm. The display of tunable emission spans the entire visible region of the spectrum. Both show temperature dependent emission and no further tuning was seen upon changing the excitation wavelength. Figure 13 shows the excitation and emission spectra for bppAu$(PVP)_n$Cl at RT. As can be seen, it exhibits a broad emission band with blue luminescence at λ_{max}=480nm. This sample has no luminescence at 77K. Figure 15 and 16 shows the excitation and emission spectra for ClAudipy and dipyAu$(PVP)_n$Cl at 77K respectively. ClAudipy has two very resolved peaks at 470nm (major) and 440nm (minor) exhibiting light blue luminescence (figure 15) while dipyAu$(PVP)_n$Cl has peak maxima at 450nm and 468nm using 300nm excitation. This emission shifts slightly upon varying the excitation to 360nm to 440nm and 468nm respectively. The two samples do not have RT emission possibly due to thermal quenching of the luminescence. The slight blue shift emission (figure 16) on the minor shoulder (440nm) indicates excitation dependent emission. The broad peak explains the brightness to the blue luminescence as shown in the inset picture. Figures 17 and 18 represent the excitation and emission spectra for ClAuppz and ppzAu$(PVP)_n$Cl respectively at 77K. ClAuppz has weak luminescence at 500nm while its polymer counterpart, ppzAu$(PVP)_n$Cl is blue shifted to 470nm. They both do not have luminescence at RT.

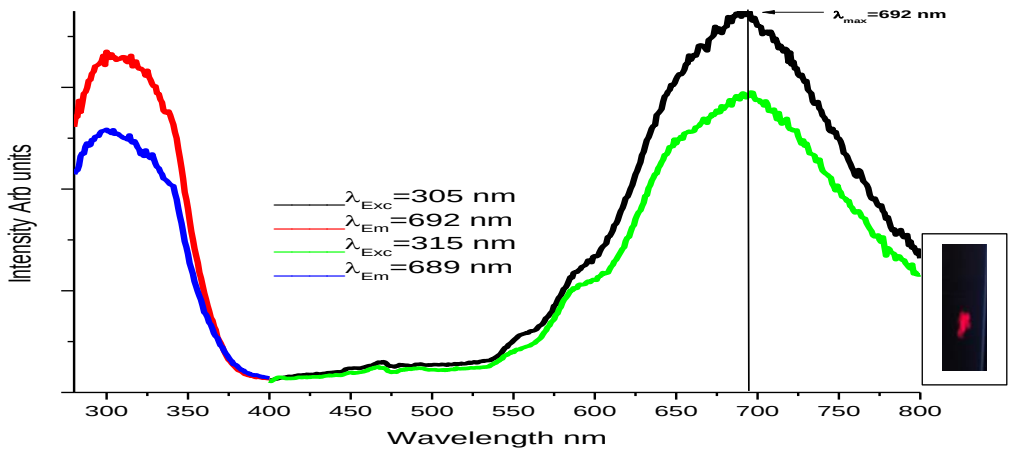

Figure 7: Excitation (left) and emission (right) spectra for ClAubpa at RT

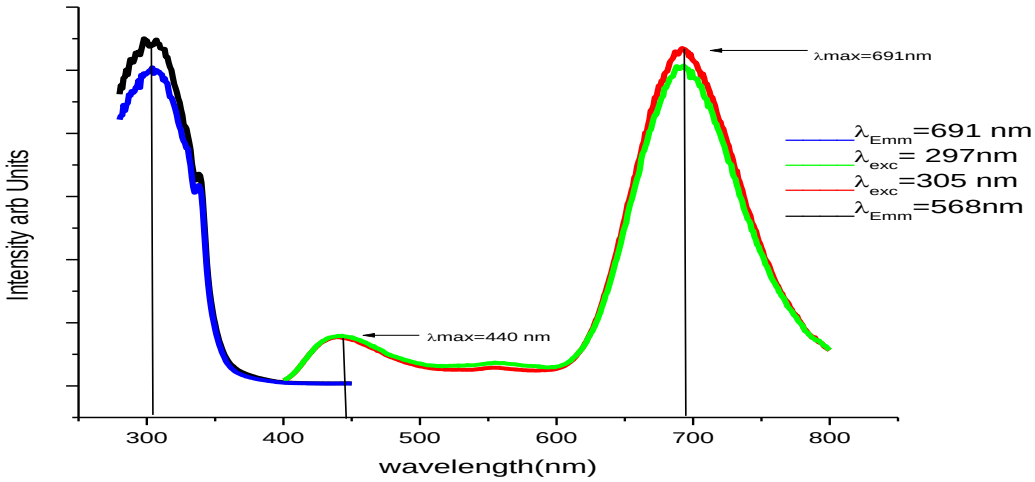

Figure 8: Excitation (left) and emission (right) Spectra for ClAubpa at 77K.

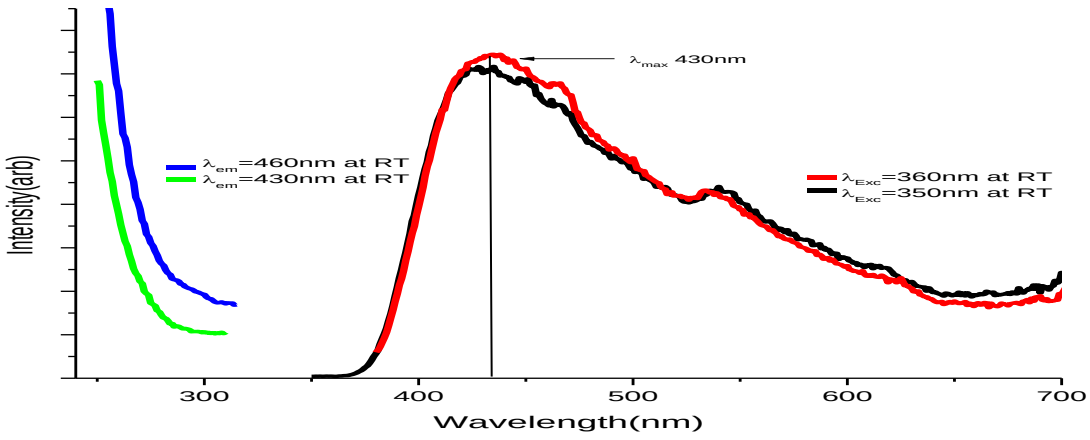

Figure 9: The photoluminescence excitation (left) and emission (right) spectra for bpaAu(PVP)$_n$Cl at RT.

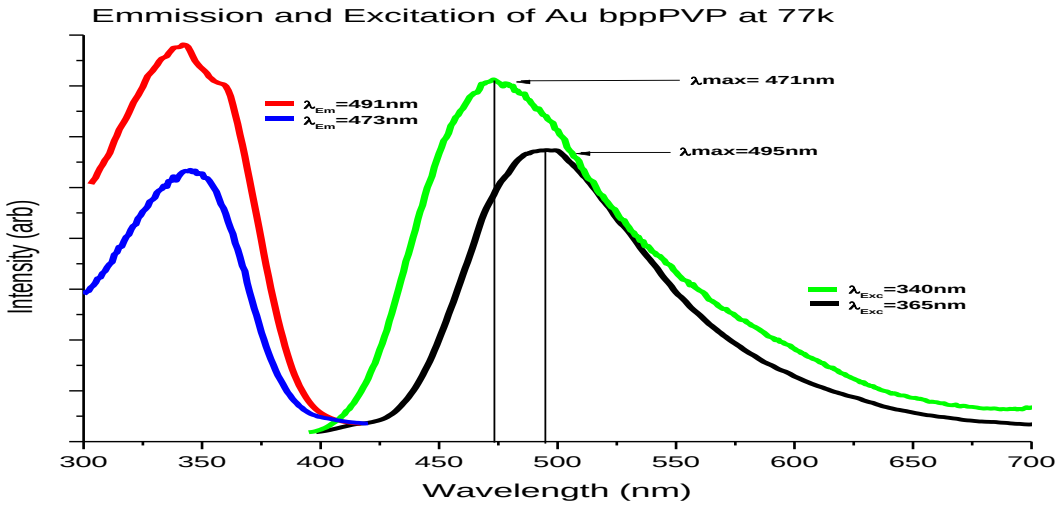

Figure 10: The steady state excitation (left) and emission (right) for bpaAu(PVP)$_n$Cl at 77K.

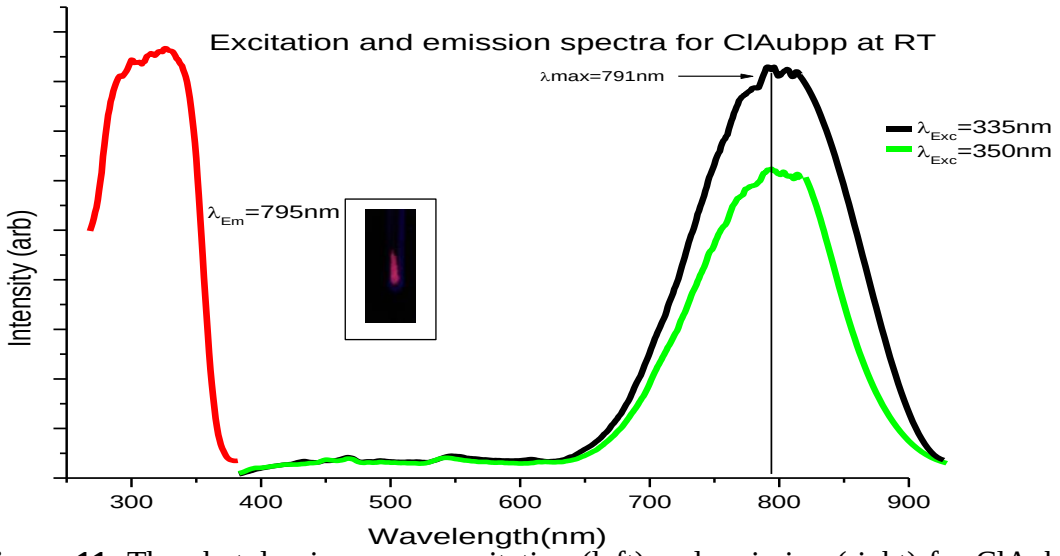

Figure 11: The photoluminescence excitation (left) and emission (right) for ClAubpp at RT showing red emission at 791nm.

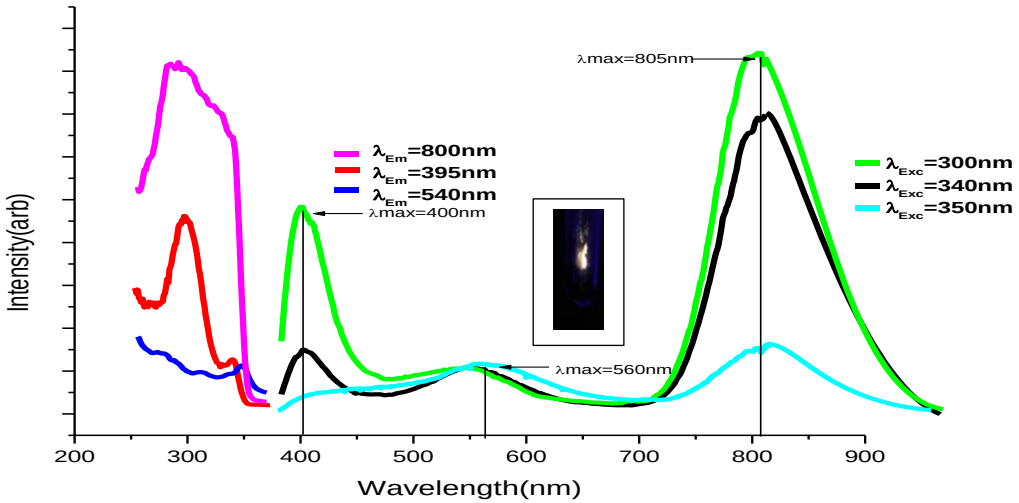

Figure12: The photoluminescence excitation (left) and emission (right) spectra for ClAubpp at 77K.

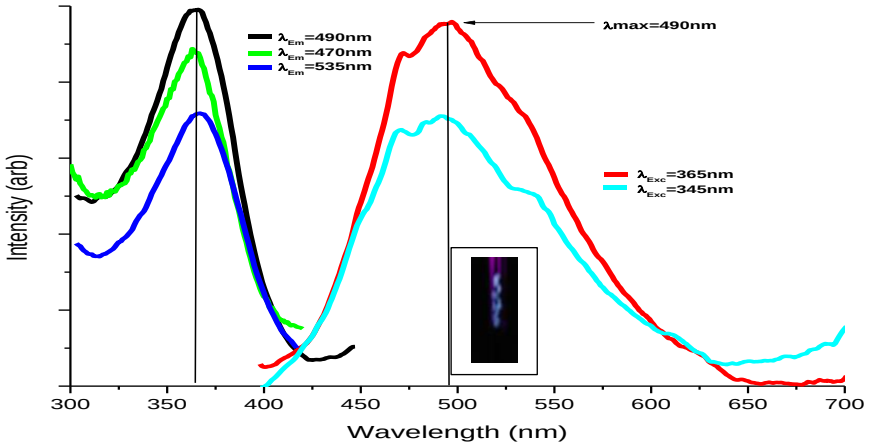

Figure 13: The photoluminescence excitation (left) and emission (right) spectra for bppAu(PVP)$_n$Cl at RT.

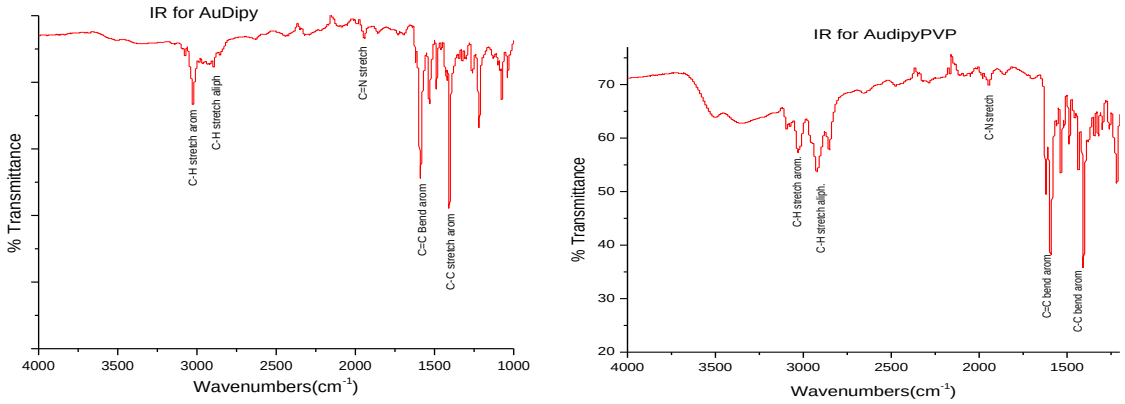

Figure 14: IR spectra for both ClAudipy (left) and DipyAu(PVP)$_n$Cl (right) confirms successful coordination of both ligands to form gold (I) complex and metallopolymer

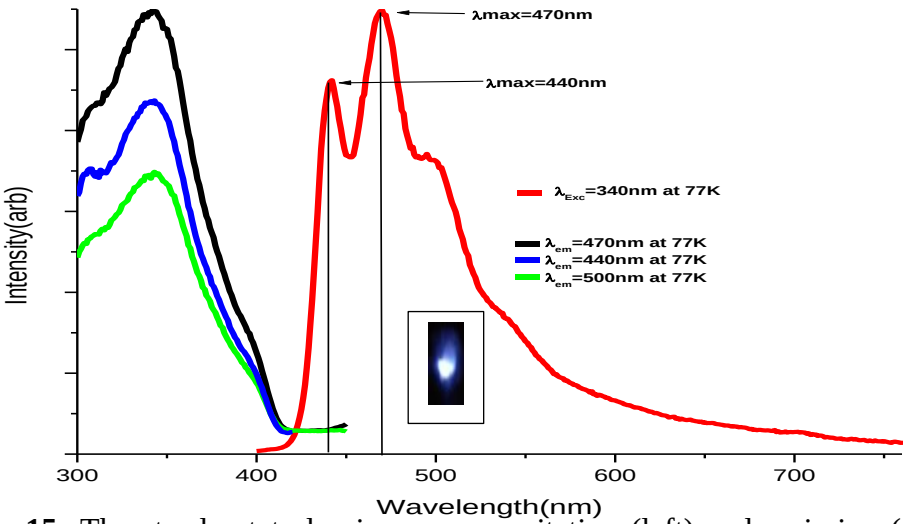

Figure 15: The steady state luminescence excitation (left) and emission (right) spectra for ClAudipy at 77K.

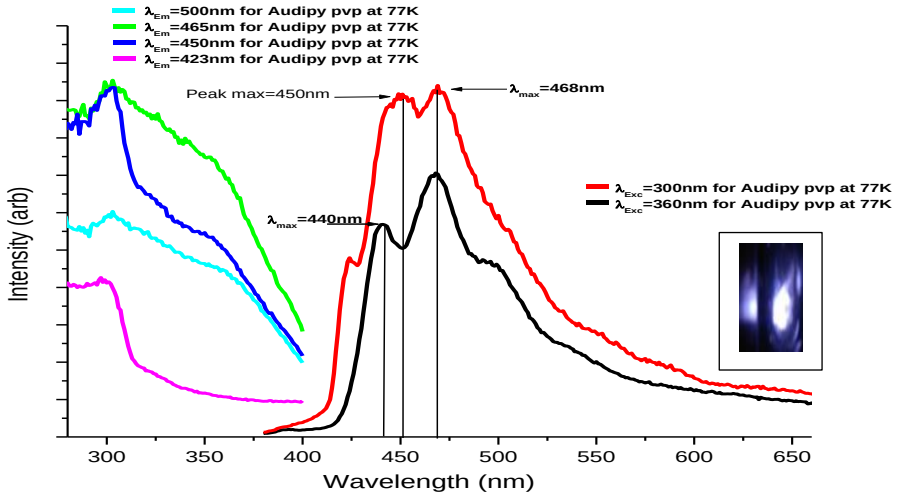

Figure 16: The photoluminescence excitation (left) and emission (right) for dipyAu(PVP)$_n$Cl at 77K showing a broad emission with two shoulders with peak maxima at 450nm and 468nm using 300nm excitation.

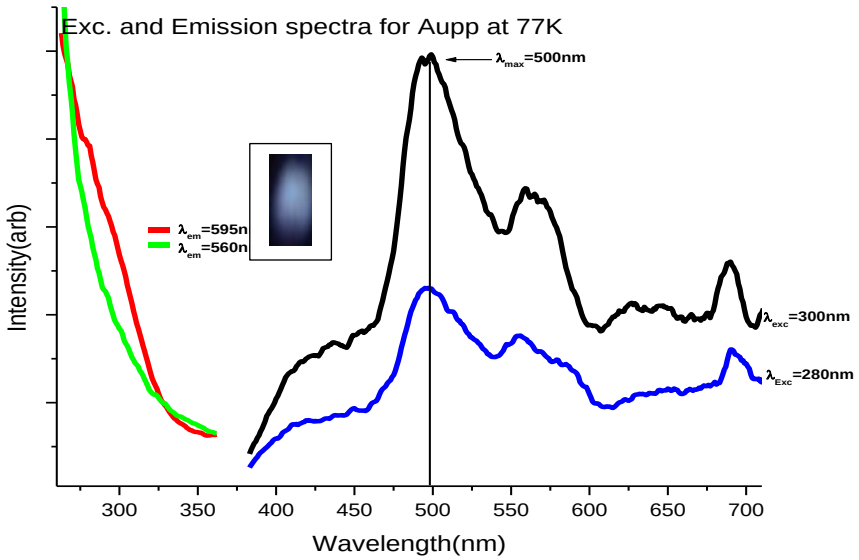

Figure 17: The photoluminescence excitation (left) and emission (right) spectra for ClAuppz at 77K.

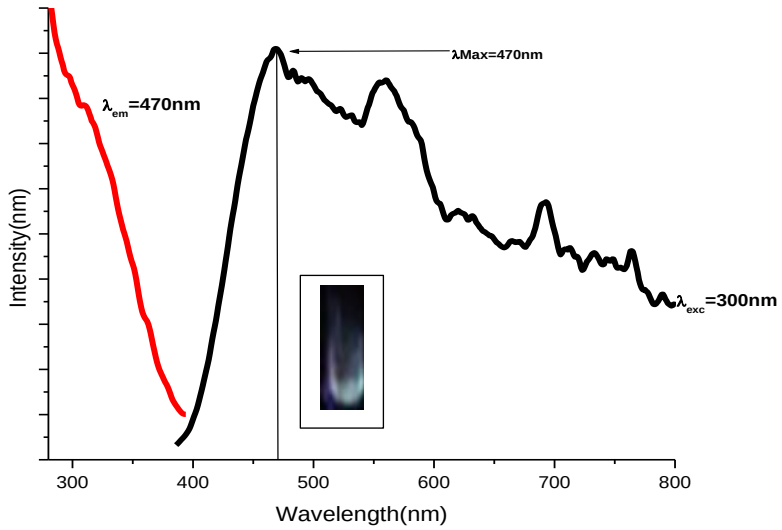

Figure 18: The excitation (Left) and emission (right) at 77K for ppzAu(PVP)$_n$Cl.

2.5 Conclusions

We were able to successfully synthesize different gold (I) complexes and characterize them using ^{1}HNMR, IR TGA, elemental analysis and UV/VIS spectrometry.

Coordination of monovalent gold (I) to different σ-donor ligands results in a new class of compounds with interesting tunable photophysical properties. With this coordination, the emission is attributed to the Au…..Au interactions[44]. Since ligands used are pyridine based, the bridge linking the pyridines plays a significant role in the overall ligand size and the geometry formed by the overall complex. The RT photoluminescence (PL) of complexes with ethane and propane linkers exhibited red luminescence with emission being red shifted as spacer length increases. Figures 7 and 11 illustrate the tunable RT emission at 692nm and 791nm respectively for ClAubpa and ClAubpp. Further tuning is achieved by cooling to 77K and introducing the polymer PVP, resulting in better resolution of emission spanning across the visible region from 400nm to 805nm (See figures 8 and 12). As would be expected, bridging ligand would affect the aurophilic interactions and the overall geometry of the complex resulting in remarkable shift in the photophysical properties. In this scenario, tuning is achievable in a variety of ways such as altering the alkane spacers, excitation wavelength and or temperature in either case. Even though conjugation is expected to enhance the luminescence, ClAubpe and bpeAu$(PVP)_n$Cl are non-luminescent both at RT and 77K possibly due to quenching.

The white emission is one of the highly sought after emissions for use in such applications that utilize full color displays. At 77K for example, ClAudipy and dipyAu$(PVP)_n$Cl display two major emission bands at λ_{max}=440nm, 470nm and λ_{max}=450nm and 468nm respectively resulting in bright white emission as shown in figures 15 and 16. On the other hand, ClAuppz and ppzAu$(PVP)_n$Cl have weak blue luminescence at 500 nm and 470nm respectively (see figure 17 and 18). The low

temperature emission may be attributed to thermal contraction resulting in excimeric Au….Au interactions. The emissions of all the gold (I) complexes present them as excellent candidates for use in different optoelectronic devices owing to their tunable emissions across the visible region of the spectrum.

We unsuccessfully made several attempts to re crystallize the complexes using different solvents with different polarities. But due to low solubility of gold (I) complexes, we were not able to obtain the crystal structure.

We introduced a polymer PVP with the aim of obtaining a novel tunable phosphorescent metal centered material. Upon introducing the PVP into the complex, blue shift emission is achieved for bpaAu$(PVP)_n$Cl and bppAu$(PVP)_n$Cl as shown in figures 9 and 13 respectively at room temperature. Both samples show blue emission at 430nm for bpaAu$(PVP)_n$Cl and 490nm for bppAu$(PVP)_n$Cl. At 77K, bppAu$(PVP)_n$Cl and dipyAu$(PVP)_n$Cl showed remarkable luminescence with temperature and excitation dependent emissions as shown in figures 9 and 16 respectively while ppzAu$(PVP)_n$Cl has a weak blue luminescence with peak maximum at 500nm as shown in figure 18.

Although introducing PVP was able to give luminescence in the range of 430-500nm at 1:1 ratio for Au: PVP: X (X=dipy, bpp or PPZ), further investigation is warranted at different ratios to not only explore the possibility of further tunable luminescence but also stability and solubility.

CHAPTER III

SYNTHESIS AND CHARACTERISATION OF MONOVALENT MIXED METAL TRINUCLEAR SILVER (I) and GOLD (I) COMPLEXES USING THE SAME AZOLATE BRIDGING LIGAND

This chapter covers the synthesis and characterization of mixed metal coinage metal trinuclear complexes involving gold (I) and Ag (I) using pyrazolate ligand. In section 3.1, we discuss the general overview of the chemistry of trinuclear coinage metal complexes. Section 3.2 discusses chemicals, materials and instruments used in the synthesis. Section 3.3 covers a detailed synthetic methods used for Au (I) and Ag (I) trinuclear complexes with the same bridging ligand. Section 3.4 covers spectroscopic findings obtained. Section 3.5 summarizes the main conclusions and findings on this work.

3.1 Introduction

The great majority of well-known developments in cyclic trinuclear complexes of the coinage metal complexes have been homometallic cyclic trimers[45, 46, and 47]. However, Burini, Fackler, and Omary groups have identified alterations in which heterometallic or stacked cyclic trimers have been isolated and structurally identified upon mixing two homometallic cyclic trimers, each with a different ligand [48, 49, and 50] to obtain a mixed metal/ligand complexes. The cyclic trinuclear silver-gold bimetallic clusters have been renowned to display amazing structural, bonding and electronic properties useful in

different applications such as catalysis[51], medicine[52], electronic devices[53] and optics because of their selectivity[54].

The suitability of transition metal complexes for use in optoelectronic applications is attributed to their phosphorescence and tunable emissions upon coordination to small molecules and polymers[55]. Previous work by Omary et al showed that pyrazolate complexes of closed- shell d^{10} elements are excellent candidates for Molecular Light Emitting Diodes (MOLEDs) [56] and it is on this backdrop that we are investigating other ligands and mixed metal moieties for enhanced emissive properties.

In this research we will focus on synthesis and characterization of a new and evolving class of fascinating complexes in which mixed-metal centers are bridged by the same azolate ligand. It is found that even submolar quantities of gold admixed with silver lead to bright emissions and increased stability despite the fact that the homometallic Ag (I) and Au (I) precursor complexes are non-luminescent. We will study the effects of increasing the number of gold atoms in the metal centers to the trinuclear complex on the photophysical properties of the complex.

3.2 Chemicals, Materials and Instrumentation.

HPLC grade benzene was purchased from sigma Aldrich and used as received. Dichloromethane (DCM) was purchased from Fisher Scientifics and used after drying using conventional methods. Silver (I) Oxide was purchased from sigma Aldrich and used as received. Standard Schlenk techniques are employed in the synthesis.

3.3 Synthesis

An approach to successful synthesis of mixed heterobimetallic gold-silver moieties will be employed to obtain organic solvent soluble material. The goal is to obtain 1:2 and 2:1 Au: Ag ratios respectively.

3.3.1 Synthesis of trinuclear silver-gold pyrazolate mixed metal complex {[3, 5-$(CF_3)_2$pz]$_3$ Ag_2Au}

ClAuTHT + {[3, 5-$(CF_3)_2$Pz] Ag}$_3$ → {[3, 5-$(CF_3)_2$pz]$_3$ Ag_2Au} denoted (Ag_2Au)

Trinuclear silver (I) pyrazolate ligand was synthesized using a literature procedure[57]. using Ag_2O (0.31g, 1.35mmol) and [3,5-$(CF_3)_2$Pz]H (0.5g, 2.45mmol. 10 ml DCM is degassed in a schlenk flask by passing a stream of purified nitrogen under ice bathe for 10 minutes. ClAuTHT (0.034g, 0.11mmol) is then added. In another schlenk flask covered with aluminum foil, {[3, 5-$(CF_3)_2$Pz] Ag}$_3$ (0.1g, 0.11mmol) is dissolved in degassed 10 ml DCM. The two solutions are mixed and stirred continuously. A white precipitate is formed after about 20 minutes. The reaction is stirred for 2 hours and the solution is removed by vacuum to obtain a white solid (yield 59.3%, M.P 110^{0}C). FTIR: ν=1600cm^{-1}(C=N stretch),ν=3050cm^{-1}(C-H aromatic). Single x- ray quality crystals were re-crystallized using DCM at 5^{0}C

3.3.2 *Synthesis of trinuclear silver- gold metal pyrazolate mixed metal complex* {[3, 5-$(CF_3)_2$pz]$_3$ Au_2Ag}

ClAuTHT + {[3, 5-$(CF_3)_2$Pz] Ag}$_3$ → {[3, 5-$(CF_3)_2$pz]$_3$ Au_2Ag} (Denoted Au_2Ag)

The procedure used in 3.3.1 is followed using 0.052g (0.16mmol) ClAuTHT and 0.1g (0.11mmol) of {[3, 5-(CF_3)2Pz] Ag}$_3$. The ratio of the starting precursors is 1:1.5. The

reaction proceeds for 2 hours. The solution remained colors and the solvent was removed by vacuum to obtain white solid. (M.P. is 115-120^{0}C- decomposes).FTIR: ν=1590cm^{-1}(C=N stretch),ν=3050cm^{-1}(C-H aromatic). X-ray quality crystals were obtained by using DCM at 5^{0}C.

3.4 Results and Discussion

Gold (I) and silver (I) are readily made by the reaction of the precursors {[3, 5-$(CF_3)_2$pz]$_3$ Ag_3} and ClAuTHT with the focus of replacing one of the silver atoms with gold. Our aim was to obtain mixed metal centered trinuclear pyrazolate complex with the same bridging ligand. Using equimolar amounts of the starting materials resulted in {[3, 5-$(CF_3)_2$pz]$_3$ Ag_2Au}, a mixed metal complex whose crystal structure is reported herein. Upon changing the ratios of the starting materials to 1: 1.5 for Ag: Au, we were able to obtain {[3, 5-$(CF_3)_2$pz]$_3$ Au_2Ag} in good yields. Crystals were grown slowly in DCM at 5°C to obtain x-ray quality crystals whose crystal structure is reported herein.

Figure 19 shows the TGA measurements for Ag_2Au (left) and Au_2Ag (right). In each case, notice the drastic weight loss between 250^{0}C and 275^{0}C where 87% and 93% of sample is lost respectively for Ag_2Au and Au_2Ag with no weight loss after 300°C. This is suggestive of sublimation of the complex. Figure 20 shows the ^{1}HNMR spectra for the trinuclear complex Ag_2Au. The single peak at 6.68ppm is for the single proton on the pyrazolate ligand. Figure 21 and 22 shows the single crystal structures and the supramolecular structures of the complexes $AuAg_2$ (A) and Au_2Ag (B) respectively. Table 1 shows the partial data illustrating the bond lengths. The Au…Au and Au…Ag

lengths range within the van der Waals force of 3.27-3.38, suggesting the M…M interactions.

The remarkable photophysical properties of solid Ag_2Au at RT and 77K is shown in figures 23 and 24 respectively. It exhibits red luminescence at λ_{max}=712nm (figure 23) and gets coarse tuned to white luminescence at λ_{max}= 563nm, 583nm (figure 24). Figure 25 and 26 illustrate the luminescence thermochromism of Au_2Ag at RT. It exhibits deep red emission at 730nm which is a very dramatic red shift from Ag_2Au emission (figure 23). Upon cooling, the emission is blue shifted to 580nm and 650nm (figure 26)

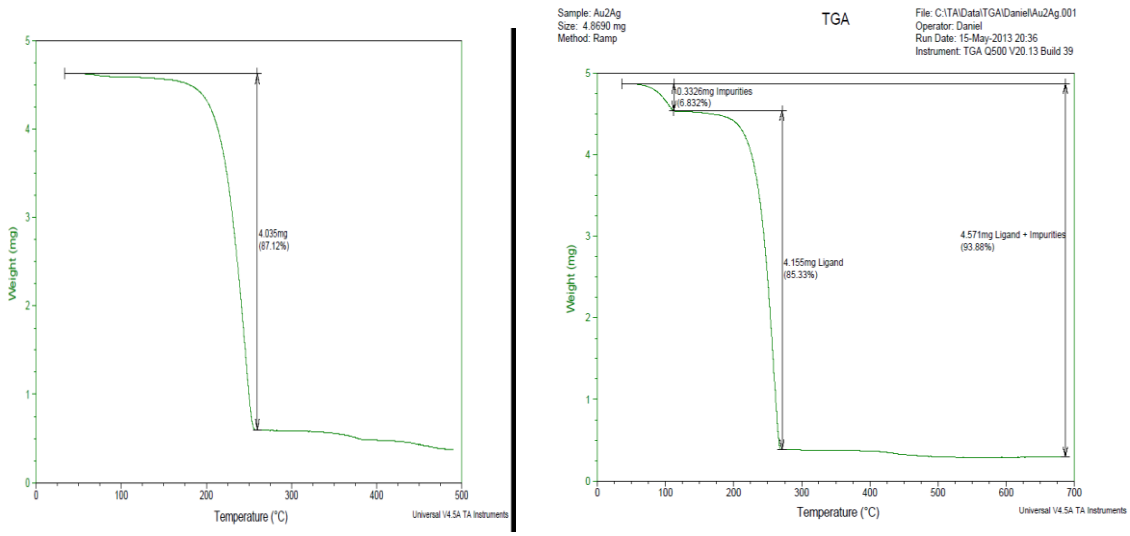

Figure 19: The TGA measurements for the {[3, 5-$(CF_3)_2$pz]$_3$ Ag_2Au} (left) complex while on the right is the figure for {[3, 5-$(CF_3)_2$pz]$_3$ Au_2Ag} complex.

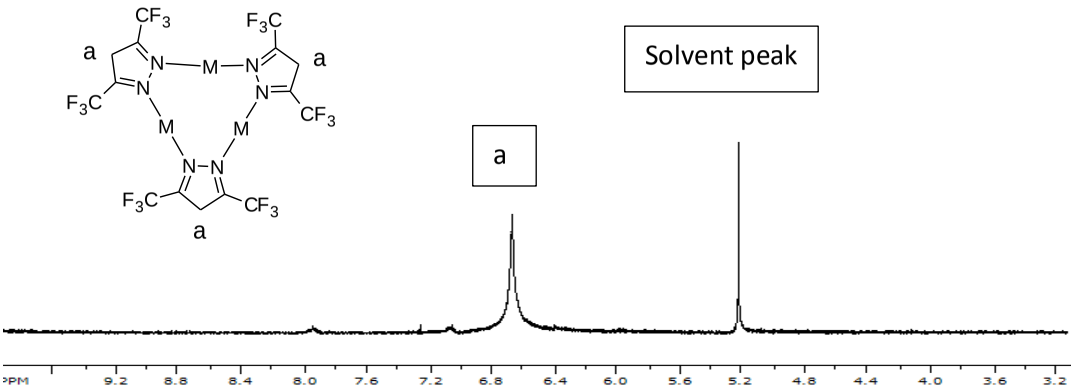

Figure 20: The ^{1}HNMR for {[3, 5-$(CF_3)_2$pz] M}$_3$ in CD_2Cl_2 where M=Ag, Au in 1:2 or 2:1 ratio for Au: Ag respectively.

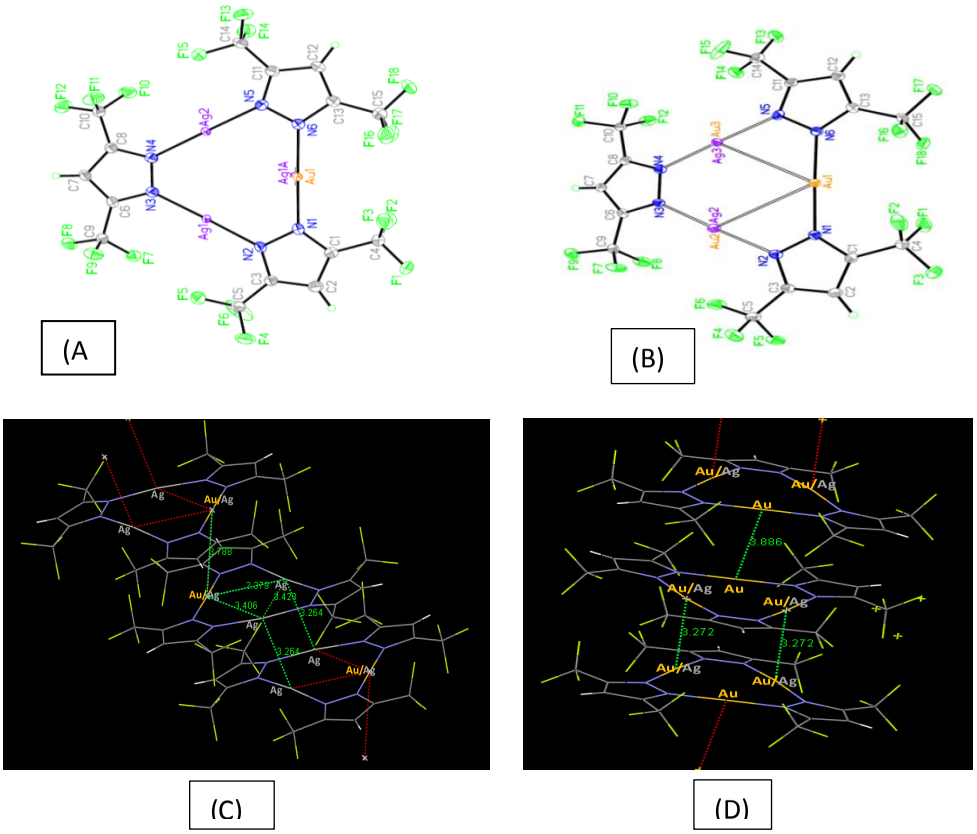

Figure 21: The crystal structure and packing shows one gold and two silver atoms in (A) and (C) for Ag_2Au with 0.43 and 0.57 probabilities for gold and silver respectively and at least 1 gold atom in (B) and (D) for Au_2Ag.

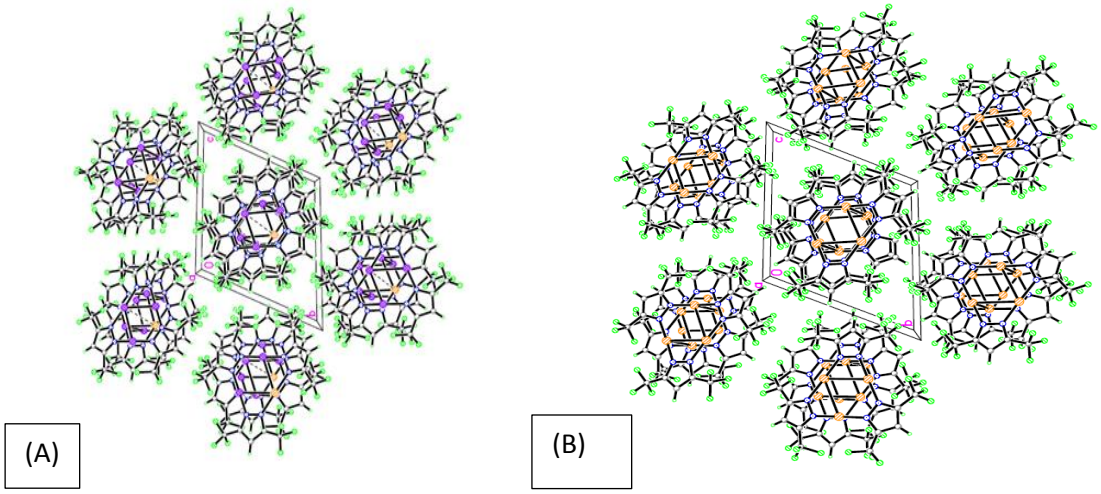

Figure 22: Diagram (A) and (B) for the crystal structure showing 1:2 and 2:1 silver: gold ratio respectively.

Table 1*:* In the tables below, (I) shows a partial data on the bond lengths Ag_2Au while (II) shows bond lengths in Au_2Ag

Bond	**Bond lengths [Å]**
Au(1)-N(6)	2.003(5)
Au(1)-N(1)	2.005(5)
Au(1)-Ag(1)	3.3780(18)
Ag(1A)-N(6)	1.995(6)
Ag(1A)-N(1)	2.013(6)
Ag(1A)-Ag(1)	3.378(4)

(I)

Bond	**Bond lengths [Å]**
Au(1)-N(1)	1.993(4)
Au(1)-N(6)	2.001(4)
Au(1)-Au(3)	3.3540(4)
Au(1)-Au(2)	3.3778(5)
Au(2)-N(3)	2.055(4)
Au(2)-N(2)	2.075(4)
Au(2)-Au(3)#1	3.2719(5)
Au(3)-N(4)	2.044(4)
Au(3)-N(5)	2.058(4)
Au(3)-Au(2)#1	3.2719(5)

(II)

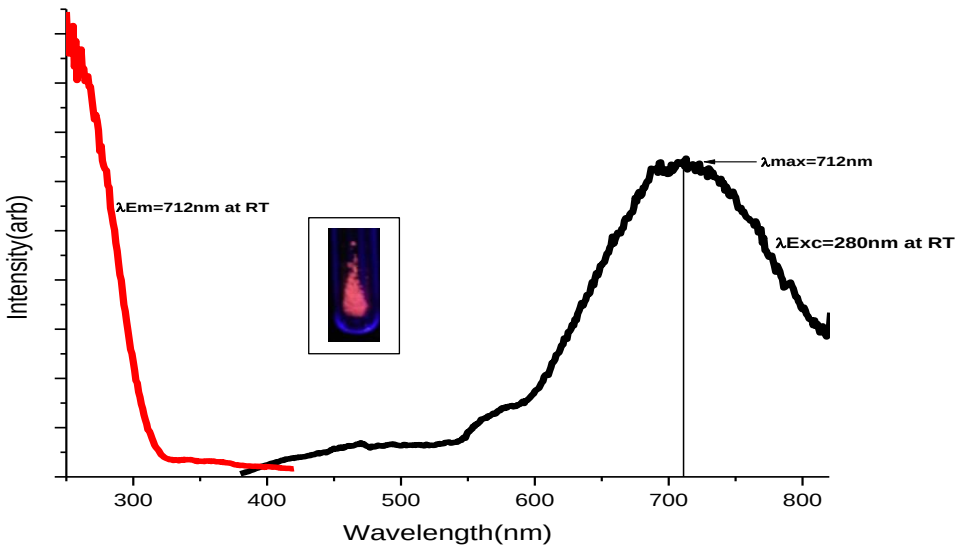

Figure 23: The photoluminescence excitation (left) and emission (right) for {[3, 5-$(CF_3)_2pz]_3$ Ag_2Au} at room temperature.

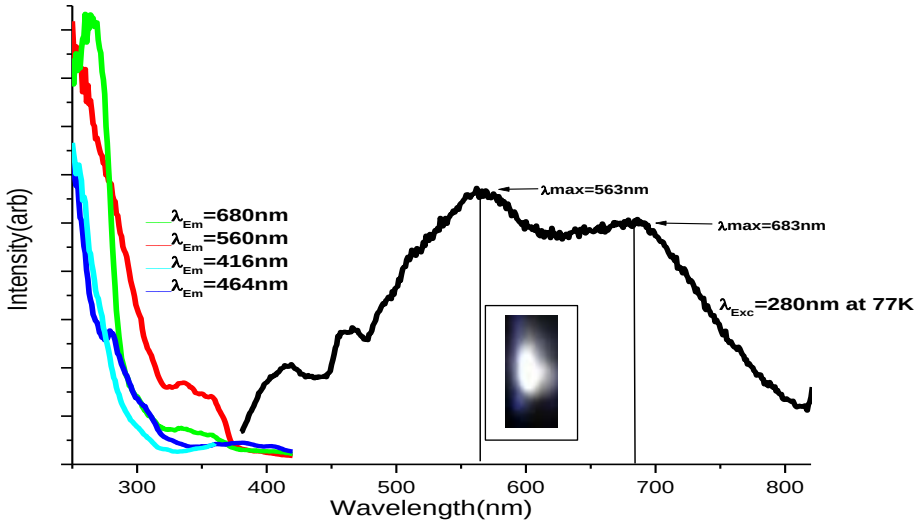

Figure 24: The excitation (left) and emission (right) for {[3, 5-$(CF_3)_2pz]_3$ Ag_2Au} at 77K

.

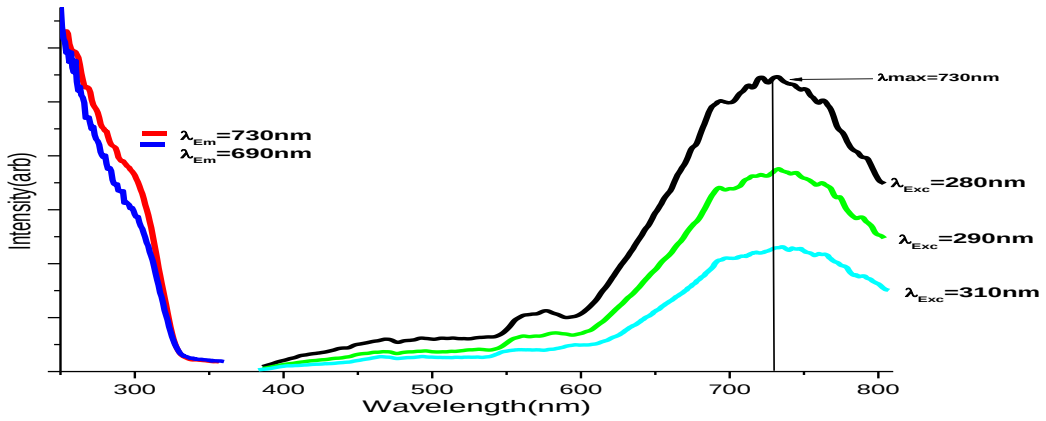

Figure 25: Photoluminescence excitation (left) and emission (right) of {[3, 5-$(CF_3)_2pz]_3$ Au_2Ag} at RT.

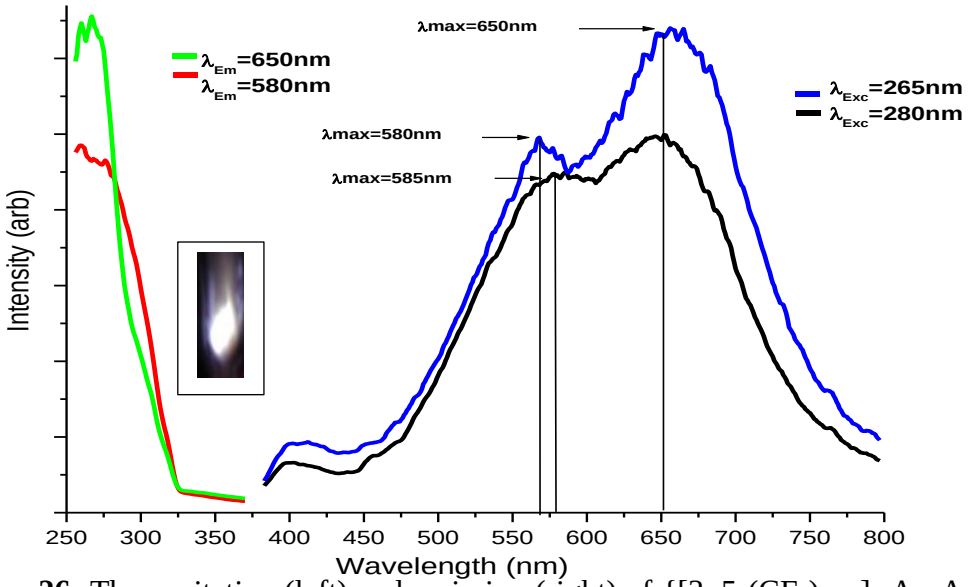

Figure 26*:* The excitation (left) and emission (right) of {[3, 5-$(CF_3)_2pz]_3$ Au_2Ag} at 77K using 1:1.5 ratio of the starting materials Au: Ag_3.

3.5 Conclusions

The silver (I) and gold (I) pyrazolato derivatives have fairly low melting points of 110°C for Ag_2Au and 115-120°C for Au_2Ag complexes respectively compared to their

homometallic analogues whose melting points are relatively high (Ag (I) and Au (I) moieties have M.P. of 212°C and 289°C respectively[57]).

Intense phosphorescence was achieved when one Au (I) ion is introduced in the trinuclear complex Ag (I) as shown in figure 23 with peak maximum at 712nm. Upon introducing two Au (I) ions in the complex, the RT luminescence is red shifted to 730nm as shown in figure 25 which falls in the intense red region in the spectrum. The red luminescence is Au-centered with interatomic Au…Au interactions while the green luminescence is Ag-centered with interatomic Ag…Ag interactions. The mixed metal Ag/Au form is mixed metal-Centered with intramolecular Ag…Au interactions. However upon heating from 77K toward RT, thermal relaxation and energy transfer pathways favor the Au-centered emission because these are non-radiative pathways that progress in the direction of the lowest-emission state hence the red luminescence at RT and white at 77K. Whereas at 77K, a combination of the three emission bands produces white emission (red + Blue+ Green= White) a physical mixture would not have allowed this since green is produced by intramolecular interactions.

In figure 25, bright white photoluminescence with two peaks at 563nm and 683nm while in figure 26 the emission is red shifted to 580nm and 650 nm respectively indicating that not only does gold un-silence the non-luminescent Ag (I) starting material at RT, but that the increase in the number of Au (I) atoms in the trimer red shifts the emission at both RT and 77K.

CHAPTER IV

STUDIES ON THE PHOTOPHYSICAL PROPERTIES OF NEW LUMINESCENT COPPER (I) AND SILVER (I) COMPLEXES

This chapter covers the photophysical studies of trinuclear complexes of Copper (I) and silver (I) containing a halide at the pyrazolyl ring 4-positions. In section 4.1, we discuss the introduction to the chemistry of the metal pyrazolate adducts of the type {[4-X-3,5-$(CF_3)_2$pz]M_3}(X=Cl or Br, M=Ag or Cu). Section 4.2 discusses the instrumentation, chemicals and materials used in the Photophysical studies. In section 4.3 we present detailed results on the photophysical studies while section 4.4, covers a summary of the conclusions.

4.1 Introduction

The first report on trinuclear complexes of fluorinated pyrazolates of copper (I) and silver (I) was made by Dias and the coworkers in the 90s[57] triggering an increase in the interest on coinage metal chemistry involving fluorinated pyrazolate ligands.

Recent studies by Omary and coworkers found that at cryogenic temperatures, fluorinated copper (I) pyrazolate complex showed bright orange luminescence while silver (I) has no luminescence[58]. Studies show for instance that even when bulky substituents are introduced on the 3- and 5- positions on the silver (I) pyrazolate ligand, structural stabilities are still maintained[59]. It has been reported that trinuclear complexes of coinage metals exhibit fascinating π-acid/base properties upon exposure to benzene and its methylated derivatives[60 (a), (b)]. In the US for example, exposure to VOCs is heavily

regulated for the reason that they are hazardous, while others such as benzene are carcinogenic[61]. Recently, however, great progress was made in studies on potential sensors for Volatile Organic Compounds (VOCs) by use of luminescent materials[62] when Rawashdeh-Omary et al found that trinuclear silver (I) pyrazolate complex has selective on/off luminescence sensing of VOCs such as benzene, Toluene and mesitylene.

Since the photophysical properties are strongly dependent on the nature of the metal, the ligand, and substituent groups around the ligand, it would be interesting to make and study the effects of replacing the only hydrogen on the pyrazolate ligand by a halogen[63]. Dias and the group at UT Arlington synthesized the halogenated pyrazolate ligand by replacing the hydrogen on 4-position with a halogen (Br or Cl).

In this work we undertake a systematic effort to study photophysical properties of perhalogenated trinuclear Copper (I) and silver (I) pyrazolato (e.g. [M (4-X-3, 5-$(CF3)_2$Pz]3 with X = Cl or Br) complexes aimed at designing a new class of sensors of VOCs such as benzene, toluene and mesitylene.

M= Cu, Ag

X= Cl, Br

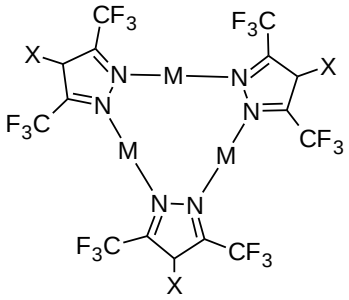

Figure 27: The general molecular structure of the halogenated trinuclear pyrazolate complex of a coinage metal.

4.2 Chemicals, Materials and Instrumentation

Excitation and emission spectra were made using a PTI QuantaMaster Model QM-3/2006SE scanning Spectrofluorometer furnished with a 75-watt xenon lamp, the excitation and emission monochromators, excitation correction unit and a PMT detector. The emission spectra were corrected for the detector wavelength-dependent response. The excitation spectra were also corrected for the wavelength-dependent lamp intensity. Temperature-dependent studies (77 K) were acquired using liquid nitrogen as a coolant in a quartz flask. Lifetime data were acquired using a high speed pulsed xenon lamp source interfaced to the PTI instrument along with an autocalibrated "Quadrascopic" monochromators for excitation wavelength selection.

4.3 Results and Discussions

The photophysical properties of $\{[4\text{-Br-3,5-}(CF_3)_2Pz]Cu\}_3$ denoted Cu_3Br and $\{[4\text{-Cl-3,5-}(CF_3)_2Pz]Cu\}_3$ denoted Cu_3Cl are investigated in this section with the general structure shown in figure 27. Figures 28, 29 and 30 show a general summary of the photoluminescence excitation and emission spectra for the solid at Room Temperature (RT) and 77K. Both samples show strongly yellow emission with peak maxima near 580nm at 77K and near 570nm at RT with very large stokes shift and unstructured emission indicative of intermolecular excitation behavior. According to literature reports, structured profile is a characteristic of excited monomer of trimer[64]. There is a notable red and blue shift for the emission and excitation peaks respectively upon cooling from the room temperature to 77K which suggests a higher degree of thermal contraction in the intermolecular exciton than the ground state moiety.

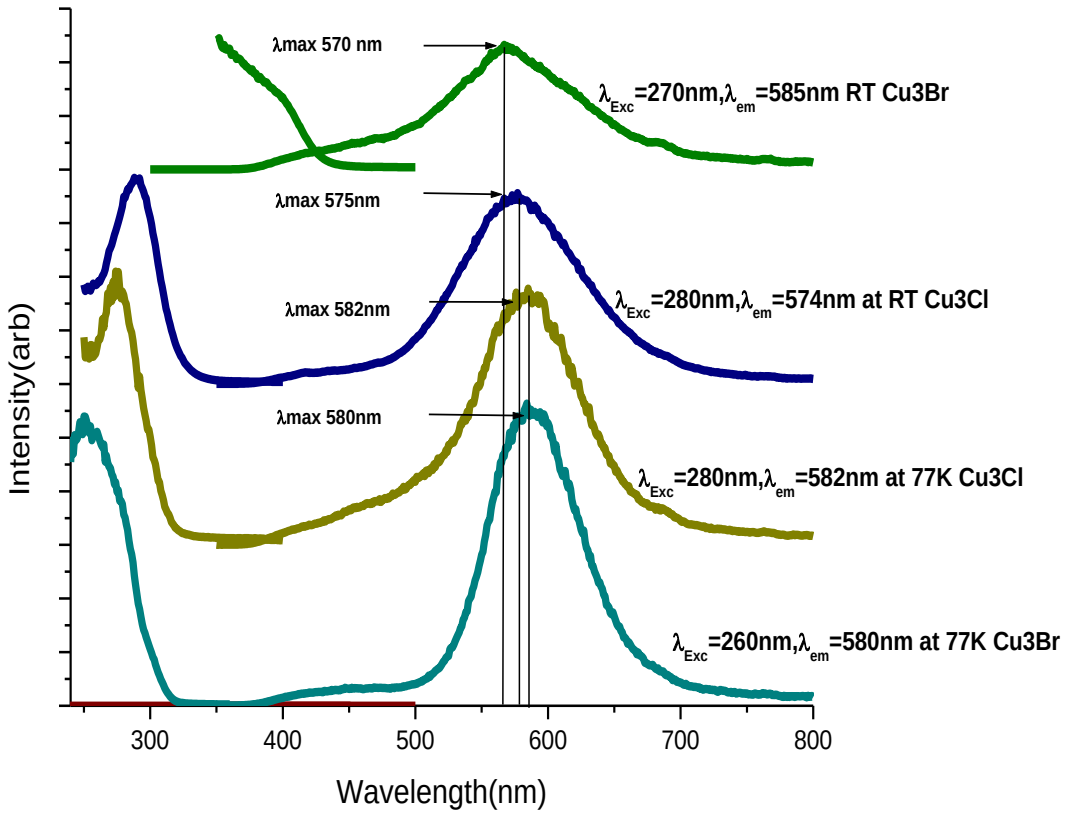

Figure 28: The photoluminescence excitation (left) and emission (right) for {[4-Br-3,5-$(CF_3)_2$Pz]Cu}$_3$ denoted Cu_3Br and {[4-Cl-3,5-$(CF_3)_2$Pz]Cu}$_3$ denoted Cu_3Cl at RT and at 77K.

The use of bromide or chloride on the pyrazolate ligand does not significantly affect the photophysical properties of trinuclear copper (I). Also, the temperature does not have a significant effect on the emission as it stays yellow at both RT and 77K.

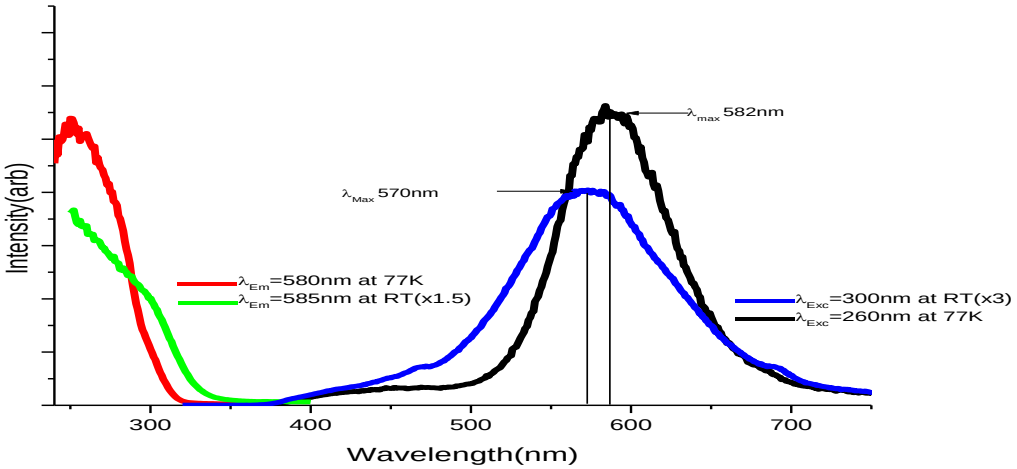

Figure 29: The steady- state photoluminescence excitation (left) and emission (right) for solid $\{[4\text{-Br-3,5-}(CF_3)_2Pz]Cu\}_3$ at RT and 77K.

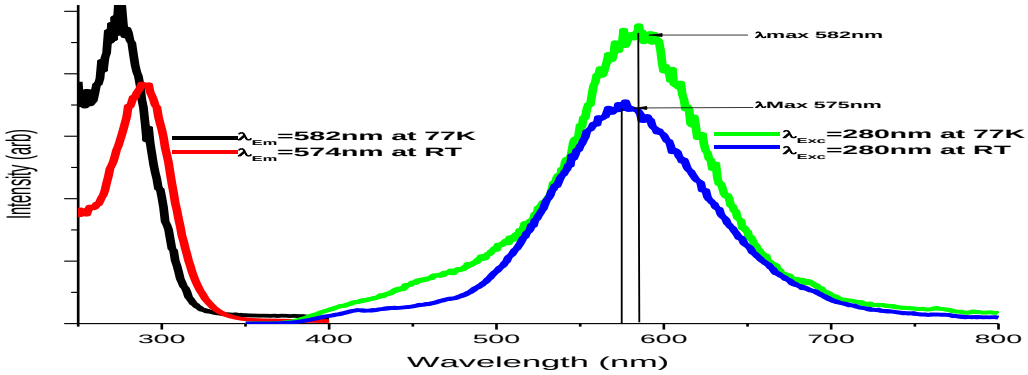

Figure 30: The photoluminescence excitation (left) and emission (right) for the solid $\{[4\text{-Cl-3,5-}(CF_3)_2Pz]Cu\}_3$ shows a bright yellow luminescence at RT (570nm) undergoing slight red shift (582nm) to a brighter yellow luminescence at 77K.

The silver complexes in figure 31 show excitation and emission spectra for $[4\text{-Cl-3, 5-}(CF_3)_2Pz]Ag\}_3$ and $\{[4\text{-Br-3,5-}(CF_3)_2Pz]Ag\}_3$ at RT and 77 K. Both samples exhibit weak blue emission near 470nm at RT. Tunable luminescence is achieved by changing

the temperature where the emission of [4-Cl-3, 5-$(CF_3)_2$Pz]Ag$\}_3$ is red shifted (480nm) upon cooling while that of {[4-Br-3,5-$(CF_3)_2$Pz]Ag$\}_3$ is blue shifted to 450nm indicating that fined emissions can be achieved at different wavelengths from 450-480nm by changing the temperature or the halogen atom at the pyrazolyl ring 4-position. The emission in all cases is weak and rather structured.

Another study on the pyrazolate ligand alone indicates that it is not luminescent at room temperature but weakly emissive at 77K (figure 32) suggesting that the emission bands of Ag (I) complexes are ligand-centered. The stokes shift are less than those of corresponding Cu(I) complexes which are respectively in the order of 10,000cm^{-1}(λ_{exc} ~ 300-350 nm) and 18,000 cm^{-1} (λ_{exc} ~ 260-280 nm), a further indication of ligand centered emission.

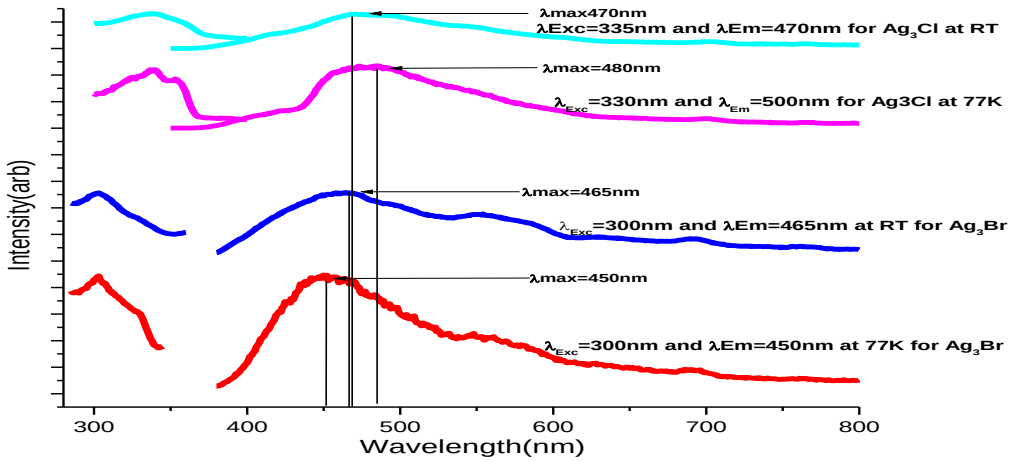

Figure 31: The photoluminescence excitation (left) and emission (right) for the solid [4-Cl-3, 5-$(CF_3)_2$Pz]Ag$\}_3$ (Ag_3Cl) and {[4-Br-3,5-$(CF_3)_2$Pz]Ag$\}_3$ (Ag_3Br) respectively at RT and 77 K.

The use of bromine as the halogen of choice produces a weak cyan color (at 450nm) at 77K, while using chlorine does show a lighter color at 480nm at 77K. RT emission is not significantly affected by halogenation with emission showing 465nm and 470nm respectively for bromide and chloride ions at the fourth position on the pyrazolate ligand.

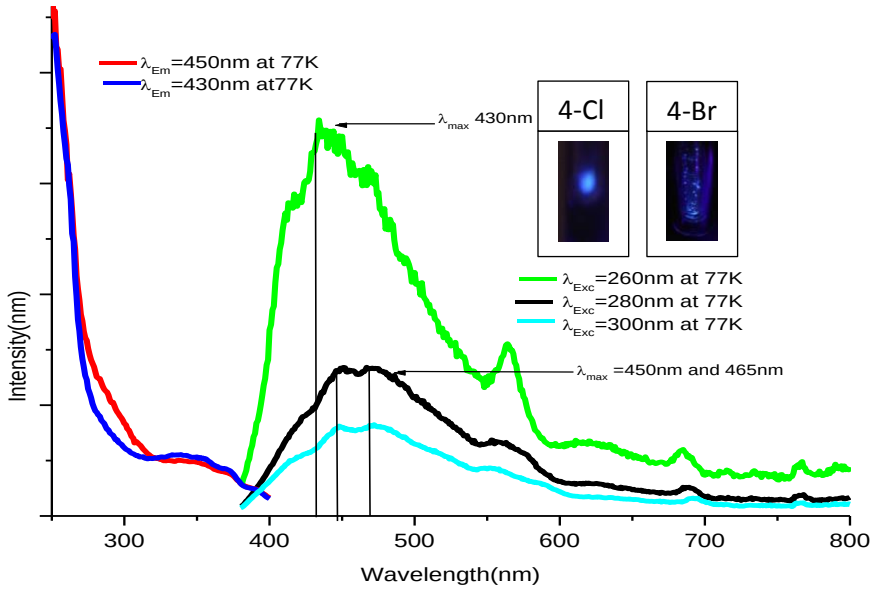

Figure 32: The photoluminescence excitation and emission spectra for the solid chlorinated pyrazolate ligand [4-Cl-3,5-$(CF_3)_2$Pz]H at 77 K.

The peak maximum at 430 nm is indicative of the blue emission. Note the red shifted emission when excitation wavelength is changed to 280nm. The photoluminescence emission for the brominated analogue is weakly blue as shown in the inset picture.

The emission of the thin films of {[4-Cl-3, 5-$(CF_3)_2$Pz]Cu}$_3$ and {[4-Br-3,5-$(CF_3)_2$Pz]Cu}$_3$ are similar to those of the corresponding solids. Upon VOC vapor exposure to the thin films of both materials, there is a remarkable color change in the

emission indicating a sensor potential. Figures 33 and 34 show that introducing the vapor of benzene to [4-Cl-3,5-$(CF_3)_2$Pz]Cu$\}_3$ and {[4-Br-3,5-$(CF_3)_2$Pz]Cu$\}_3$ results in a dramatic shift in emission from bright yellow with no vapor to green in the presence of benzene vapor. In figures 35 and 36 the same behavior using toluene on both materials is seen. In both cases, the emission maxima are blue shifted from 580nm for a dry sample to about 560nm in the presence of the vapor. On the other hand, mesitylene shows a quenching on both samples as shown in figures 37 and 38 with the yellow emission of the copper trimer fading almost completely in the first 20 minutes of exposure.

The luminescence vapochromism exhibited by the Cu (I) complexes are fully reversible. In the presence of the VOC, the emission is green and when the vapor is removed using heat, vacuum or air, the original bright yellow emission is obtained. Control experiments using aliphatic VOCs did not yield a color change suggesting selectivity of the emission. On the other hand, [4-Cl-3,5-$(CF_3)_2$Pz]Ag$\}_3$ and {[4-Br-3,5-$(CF_3)_2$Pz]Ag$\}_3$ did not show luminescence vapochromism.

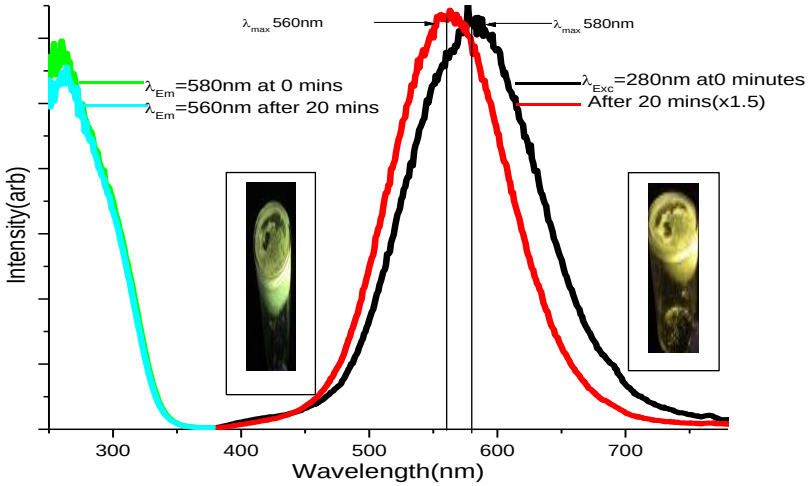

***Figure 33*:** The photoluminescence excitation (left) and emission (right) for {[4-Cl-3, 5-$(CF_3)_2$Pz]Cu}$_3$ under benzene (vapor) at RT

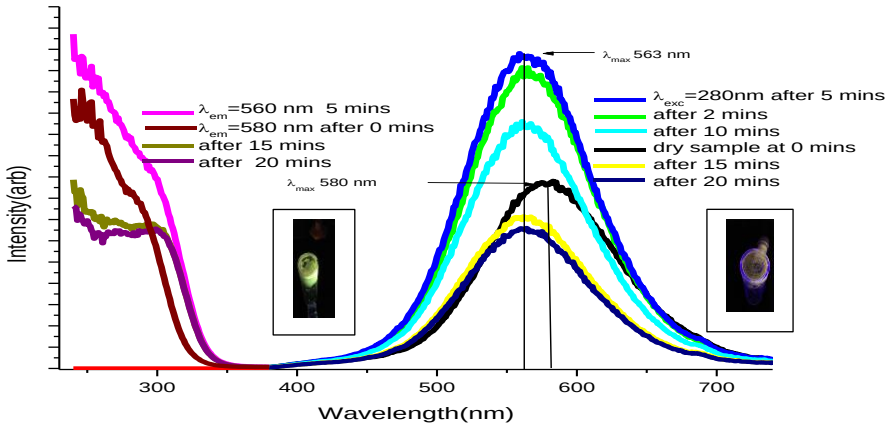

Figure 34: The photoluminescence excitation (left) and emission (right) spectra for the thin film of {[4-Br-3, 5-$(CF_3)_2$Pz]Cu}$_3$ before and after exposure to benzene vapor.

Dry Chlorinated trinuclear copper (I) pyrazolate complex shows a yellow luminescence (580nm) undergoing luminescence vapochromism giving green emission (560nm)

achieved within 2 minutes after exposure. Similarly, dry Cu_3Br has yellow luminescence (580nm) and upon exposure, light green emission is achieved at 563nm within 2 minutes. After 10 minutes, the emission weakens considerably without further change after 20 minutes.

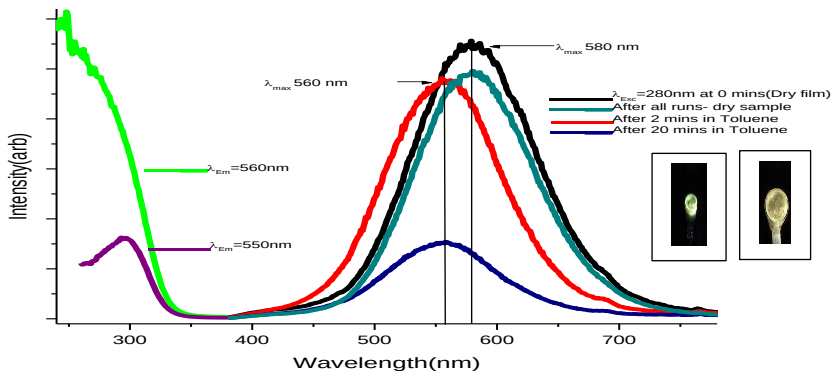

Figure 35: The excitation (left) and emission (right) representing luminescence vapochromism for $\{[4\text{-Cl-3, 5-}(CF_3)_2Pz]Cu\}_3$ in Toluene vapor.

The dry thin film (580nm) undergoes a 20nm blue shift to give green luminescence (560nm). The shift was achieved within the first two minutes of exposure to toluene vapor followed by a progressive decrease in the intensity as seen after 20 minutes.

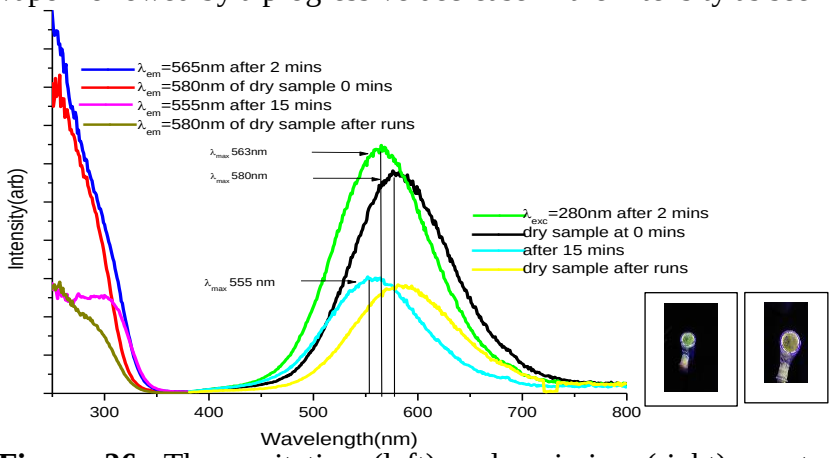

Figure 36: The excitation (left) and emission (right) spectra showing luminescence vapochromism of the thin film of $\{[4\text{-Br-3, 5-}(CF_3)_2Pz]Cu\}_3$ in toluene vapor.

Dry film has yellow emission at 580nm and shifts to green luminescence at 563nm upon contact with the vapor after 2 minutes. Progressive shifting in emission is seen after 15 minutes (555nm). Reversibility of the photophysical properties is achievable as depicted by the dried sample which shows the emission at 580nm.

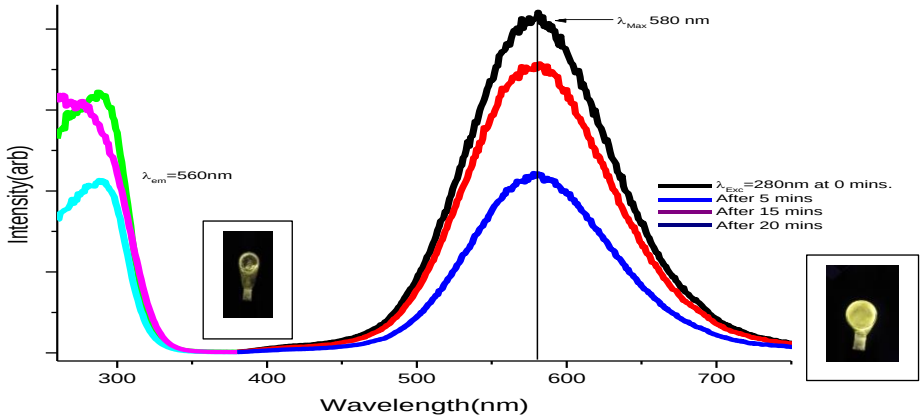

Figure 37: The photoluminescence excitation (left) and emission (right) spectra for {[4-Cl-3, 5-$(CF_3)_2$Pz]Cu}$_3$ in mesitylene vapor.

The film displays progressive quenching with no notable shift in emission. The intensity decreased very significantly after the first 20 minutes of exposure to the vapor

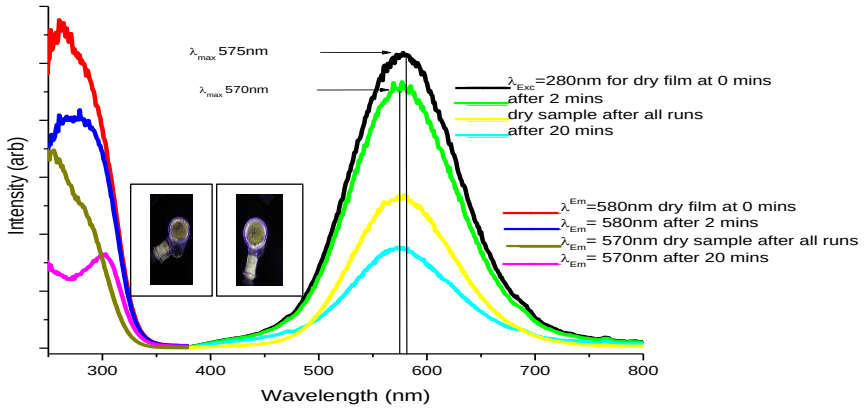

Figure 38: The photoluminescence excitation (left) and emission (right) of the thin film of {[4-Br-3, 5-$(CF_3)_2$Pz]Cu}$_3$ under mesitylene vapor.

4.4 Conclusions

This study provides understanding on structure and the photoluminescence properties of $\{[3,5\text{-}(CF_3)_2,4\text{-}(X)Pz]M\}_3$, where X = Cl or Br and M = Cu or Ag. Whereas trinuclear complexes of Cu (I) or Ag (I) with 4-H exhibit metal-metal interactions (~3.6Å), the four complexes in this study instead exhibited metal-halogen interaction (>5 Å). The metal-metal interaction which plays a critical role in the photoluminescence properties of trinuclear pyrazolate complex with 4-H

The emission bands of solid Ag_3Cl and Ag_3Br have weak emission at peak maxima at 470nm and 465nm respectively at RT. This corresponds with a weak cyan color in the spectrum. The Ag_3Br however undergoes a blue shift at 77K with blue emission peak at 450nm while Ag_3Cl undergoes a red shift to give green emission at 500 nm. In either case, the Ag_3Cl seems to higher wavelength emission (470nm and 500nm) than Ag_3Br which has emission bands at 465nm and 450nm respectively at RT and 77K.

The Cu_3Cl and Cu_3Br have yellow RT luminescence at 570nm and 574nm respectively. Both undergo red shift emission at 77K to give more intense yellow luminescence at 580nm and 582nm respectively for Cu3Cl and Cu3Br indicating that the type of halogen used does not significantly affect the photophysical properties of the complex. This however indicates that hydrogenless complex has a dramatic shift on the photophysical properties as compared to the hydrogenated trinuclear pyrazolate complex. While both hydrogenated complexes are fairly stable at RT, the halogenated silver decomposes only a few hours after synthesis. The Cu_3Cl and Cu_3Br are equally stable at RT.

Trinuclear copper (I) pyrazolate complex has good stability at room temperature with orange luminescence but no luminescence vapochromism to benzene and its methylated derivatives while the Ag (I) pyrazolate is non-luminescent but exhibits on/off green luminescence vapochromism to benzene and its methylated derivatives[65]. The halogenated Cu (I) pyrazolates have high sensitivity (2minutes) showing green luminescence thermochromism to benzene and toluene while mesitylene has quenching effect with the emission intensity decreasing consistently with time.

REFERENCES

1. Harvey, E.N The history of Luminescence, *Am. Phil.Soc*. **1957**, Vol. 44

2. R.F. Ziolo, S. Lipton and Z. Dori, *J. Chem. Soc., Chem. Commun*., **1970**, 1124

3. Hayashi, A.; Olmstead, M. M.; Attar, S.; Balch, A. L. *J. Am. Chem. Soc.* **2002**, *124*, 5791

4. Omary, M. A.; Mohamed, A. A.; Rawashdeh-Omary, M. A.; Fackler, J. P., Jr. *Coord. Chem. ReV.* **2005**, *249*, 1372

5. Eduardo J F., Antonio L. and José M L. *Gold Bulletin* **2001**, ***34***,*1*

6. Omary, M. A.; Rawashdeh-Omary, M. A.; Gonser, M. W. A.; Elbjeirami, O.; Grimes, T.; Cundari, T. R.; Diyabalanage, H. V. K.; Gamage, C. S. P.; Dias, H. V. R. *Inorg. Chem*. **2005**, *44*, 8200

7. Rawashdeh-Omary, M. A.; Lopez-de-Luzuriaga, J.; Rashdan, M.D.; Elbjeirami, O.; Monge, M. Rodriguez-Castillo, M.; Laguna, A. *J. Am. Chem. Soc*. **2009**, 131, 3824-3825

8. Chen, X.-Y.; Yang, X.; Holliday, B. J. *J. Am. Chem. Soc.* **2008**, *130*, 1546

9. Shaw, C. F., III. The Biochemistry of Gold. In *Gold: Progress in Chemistry, Biochemistry and Technology*; Schmidbaur, H., Ed.; Wiley: Chichester, New York, 1999, Chapter 10

10. Blonder, R.; Levi, S.; Tao, G.; Ben-Dov, I.; Willner, I. *J. Am. Chem. Soc.* **1997**, *119*, 10467

11. Wolf, M. O.; Fox, M. A. *J. Am. Chem. Soc.* **1995**, *117*, 1845

12. Mansour, M. A.; Connick, W. B.; Lachicotte, R. J.; Gysling, H. J.; Eisenberg, R. *J. Am. Chem. Soc.* **1998**, *120*, 1329

13. Vickery, J. C.; Olmstead, M. M.; Fung, E. Y.; Balch, A. L. *Angew. Chem., Int. Ed. Engl.* **1997**, *36*, 1179

14. J.M. Forward, J.P. Fackler, Jr. and Z. *Assefa, in 'Optoelectronic Properties of Inorganic Compounds'*, ed. D. M. Roundhill And J.P. Fackler, Jr., Plenum Press, New York, **1999**, pp. 195-226

15. (a) Draws, C. A.; Exstrom, C. L Sowa, J. R.; Jr.; Mann, K. R.; *Chem. Mater*. **1997**, 9, 363
(b) Mansour, M. A.; Connick, W, B.; Lachicotte, R. J.; Gysling, H.J.; Eisenberg, R. *J. Am. Chem. Soc.* **1998,** 120, 1329**.**
(c) Vickery, J. C.; Olmstead, M. M.; Fung, E. Y.; Balch, A. L. *Angew Chem*. **1997**, 109, 1227

16. Kim, P. S. G.; Hu, Y, Brandy's, M. C.; Burchell, T. J.; Puddephatt, R. J.; Sham, T. K. *Inorg. Chem.* **2007**, 46, 949

17. Schmidbaur, H. *Gold: Progress in Chemistry, Biochemistry and Technology;* Wiley: New York, **1999**

18. Grohman, A.; Schmidbaur, H. In *Comprehensive Organometallic Chemistry II;* Abel, E. W., Stone, F. G. A., Wilkinson, G., Eds.; Elsevier: Oxford, **1995**

19. Dias. H.R. V.; Diyabalanage, H. V. K.; Rawashdeh-Omary, M.; Franzman, A. M.; Omary, M. A. *J. am. chem. soc*. **2003**,125, 12072-12073

20. Fernandez, E. J.; Lagunab, A and Lopez-de-Luzuriaga, J.M. *Gold Bulletin* **2001**, 34, 1

21. Roundhill, D. M.; Fackler, J. P.; Optoelectronic Properties of inorganic Compounds; Plenum press: New York, **1999**

22. Omary, M. A.; Rawashdeh- Omary, M. A.; Gonser, M. W.; Elbjeirami, O.; Grimes, T.; Cundari, T. R.; Diyabalanage, H. V.; Gamage, C.S.; Dias. H. V.; Inorg. Chem **2005**, 44, 8200-8210

23. Pyykko¨, P. *Chem. Rev.* **1997**, *97*, 597

24. Schmidbaur, H. *Chem. Soc. Rev*. **1995**, 391

25. Ferna´ndez, E. J.; Lo´pez-de-Luzuriaga, J. M.; Monge, M.; Rodrı´guez, M. A.; Crespo, O.; Gimeno, M. C.; Laguna, A.; Jones, P. G. *Inorg. Chem.* **1998**, *37*, 6002

26. Forward, J. M.; Fackler, J. P., Jr.; Assefa, Z. Photochemical Properties of Gold (I) Complexes. In *Optoelectronic Properties of Inorganic Compounds*; Roundhill, D. M., Fackler, J. P., Jr., Eds.; Plenum Press: New York, **1999**; pp 195-226

27. Pyykko, P. *Angew. Chem., Int. Ed.* **2004**, *43*, 4412

28. Canales, F.; Gimeno, M. C.; Laguna, A.; Jones, P. G. *J. Am. Chem. Soc.*, **1996**, *118*, 4839

29. Mansour, M. A.; Connick, W. B.; Lachicotte, R. J.; Gysling, H. J.; Eisenberg, R. J. *J. Am. Chem. Soc.* **1998**, *120*, 1329

30. Dziwok, K.; Lachmann, J.; Wilkinson, D. L.; Müller, G.; Schmidbaur, H. *Chem. Ber.* **1990**, *123*, 423

31. Rawashdeh-Omary, M. A.; Omary, M. A.; Patterson, H. H,; Fackler, J. P. *J. of Am. Chem. Soc.* **2001**, 123, 11237-11247

32. Pyykko¨, P.; Zhao, Y.-F. *Angew. Chem.* **1991**, *103*, 622

33. Rawashdeh-Omary, M. A.; Omary, M. A.; Patterson, H. H.; Fackler, J. P. *J. Am. Chem. Soc.* **2001**, *123*, 11237

34. Furuta, P. T.; Deng, L.; Garon, S.; Thompson, M. E.; Frechet, J. M. J. *J. Am. Chem. Soc.* **2004**, *126*, 15388

35. Rawashdeh-Omary, M. A.; Omary, M. A.; Patterson, H. H.; Fackler, J. P. *J. Am. Chem. Soc.* **2001**, 123, 45

36. Wolf, M. J. Inorg. and Organometallic polymers and materials **2006**, 16, 189-199

37. Eloi, J.; Chabanne, L.; Whittell, R. G.; Manners, I. *Materials today*, **2008**, 11, 4

38. Furuta, P. T.; Deng, L.; Garon, S.; Thompson, M. E.; Frechet, J. M. J, *J. Am. Chem*. Soc. **2004**, 126, 15388-15389

39. Knapton, D., *et al.*, *Macromolecules* **2006**, 39, 651

40. Dobrawa, R., *et al.*, *Macromolecules* **2005** 38, 1315

41. Uson, R.; Laguna, A.; Laguna, M. *Inorganica Chimica Acta* **1979**, 182, 449-454

42. Uson, R.; Laguna, A.; Brun, P. *J. organometallic Chem*. **1979,** 182, 449-454

43. Uson, R.; Laguna, A.; Vincente, J. J. organometallic chem. **1977**, 131, 471-475

44. Roundhill, D. M.; Fackler, J. P., Jr. *Optoelectronic Properties of Inorganic Compounds*; Plenum: New York, **1999**; Chapter 6

45. Omary, M. A.; Mohamed, A. A.; Rawashdeh-Omary, M. A.; Fackler, J. P., Jr. *Coord. Chem. Re*V. **2005**, *249*, 1372

46. Burini, A.; Mohamed, A. A.; Fackler, J. P., Jr. *Comments Inorg. Chem.* **2003**, *24*, 253

47. Hayashi, A.; Olmstead, M. M.; Attar, S.; Balch, A. L. *J. Am. Chem. Soc.* **2002**, *124*, 5791

48. A. A. Mohammed, R. Galasi, F. Papa, A. Burini, J. P. Fackler Jr. *Inorganic Chem*. Vol. 45, No. 19. **2006** 7771

49. A. A. Mohammed, A. Burini, J. P. Fackler Jr. *J. Am. Chem. Soc*. **2005**, 127, 5012-5013

50. Omary, M. A, Rawashdeh-Omary, M. A, Gonser, Elbjeirami, O, Grimes, T, Cundari, T. R, Diyabalanage, H. V. K, Gamage, C. S P, Dias, H. V. K, *Inorg. Chem*. Vol. 44, No. 23, **2005**

51. Adams, R. D.; Captain, B. *J. Organomet. Chem*. **2004**, *689*, 4521-4529

52. Lopez, N.; Norskov, J. K. *J. Am. Chem. Soc.* **2002**, *124*, 11262

53. *Optoelectronic Properties of Inorganic Compounds*; Roundhill, D. M., Fackler, J. P., Jr., Eds.; Plenum Press: **1999**, New York

54. Rousset, J. L.; Aires, J. C. S.; Sekhar, R.; Me´linon, P.; Prevel, B.; Pellarin, M. *J. Phys. Chem. B* **2000**, *104*, 5430

55. C. Yang, M. Messerschmidt, C. Coppens, M.A. Omary, Inorg. Chem. **2006**, 45, 6592

56. Omary, M.A.; Rawashdeh-Omary, A. M.; Diyabalanage, H. V.K.; Dias. H.R. V *Inorg. Chem*. **2003**, 42, 2

57. Dias, H. V. R.; Polach, S. A.; Wang, Z. *J. Fluor. Chem.* **2000**, *103*,163

58. M. A. Omary, M. A. Rawashdeh-Omary, M. W. A. Gonser, O. Elbjeirami, T. Grimes, T. R. Cundari, H. V. K. Diyabalanage,C. S. P. Gamage and H. V. R. Dias, Inorg. Chem., **2005**, 44, 8200

59. Dias, H. V. R, Gamage, C. S, Kelter, J, Diyabalanage, H. V. K, Omari, I, Eyobo, Y, Dias, N. R, Roehr, N, McKinney, L, Poth, Theresa, *Inorg. Chem***.,** Vol. 46, No. 8, **2007** 2979

60. (a)Omary, M. A.; Mohamed, A. A.; Rawashdeh-Omary, M. A.; Fackler, J. P. *Coord. Chem. Re*v. **2005**, *249*, 1372-81.
(b)Olmstead, M. M.; Jiang, F.; Attar, S.; Balch, A. L. *J. Am. Chem. Soc.* **2001**, *123*, 3260-7

61. (CDC Web site accessed 4/26/2013)
http://www.cdc.gov/niosh/ershdb/EmergencyResponseCard_29750032.html

62. Rawashdeh-Omary, M. A.; Rashdan, M. D.; Dharanipathi, S.; Elbjeirami, O.; Ramesh, P.; Rasika Dias, H. V. *Chem. Commun.* **2011**, *47*, 1160

63. Dias, H. V. R.; Lu, H.-L. Inorg. Chem. **1995**, 34, 5380

64. Dias, H. V. R.; Diyabalanage, H. V. K.; Eldabaja, M. G.; Elbjeirami, O.; Rawashdeh-Omary, M. A.; Omary, M. A. *J. Am. Chem*. Soc. **2005**, 127, 7489-7501

65. Omary, M.A.; Rawashdeh-Omary, M. A.; Gonser, M. W. A.; Elbjeirami, O.; Grimes, T.; Cundari, T.; Diyabalanage, H.V.K.; Gamage, C.S.P.; Dias, H.V.R. *Inorg. Chem*. **2005**, 44, 23